Using Human Whole Saliva to Better Understand the Influences of Yogurt Rheological and Tribological Behaviors on Their Sensory Texture

Maryam Baniasadidehkordi and Helen S. Joyner

1 Introduction

Yogurt, a popular semisolid food in many countries, is produced by fermentation of milk using the lactic acid bacteria *Streptococcus salivarius* ssp. *thermophilus* and *Lactobacillus delbrueckii* ssp. *bulgaricus*. The demand for reduced- or non-fat yogurts has increased during recent years due to health concerns. However, reduction or removal of fat from yogurts can compromise their texture attributes, since fat plays a major role in creating a smooth, creamy texture in dairy products (De Wijk et al. 2006; Chojnicka-Paszun et al. 2012). Application of hydrocolloids has been an effective solution to improve the textural properties of reduced-fat yogurts. There are a wide range of hydrocolloids used in dairy products as fat replacers (Ognean et al. 2006; Peng and Yao 2017), including carboxymethyl cellulose (CMC), locust bean gum (LBG), and starch (Cho and Prosky 1999; Peng and Yao 2017). CMC is an anionic hydrocolloid that is used widely in dairy products as a fat replacer to enhance their textures (Cho and Prosky 1999). This gum is not only an effective stabilizer in dairy systems but also a dietary fiber with health benefits such as reduction of blood cholesterol and improvement of digestion and absorption (Cho and Prosky 1999). LBG is a galactomannan with a 1:4 ratio of galactose:mannose, and its mannan part is made soluble by side chains of single galactoses. LBG is a neutral (non-ionic) hydrocolloid that is stable at a pH range of 3.5–11 (Cho and Prosky 1999). Corn starch and potato starch with modified structures are usually used as fat mimetics in dairy products (Cho and Prosky 1999; Peng and Yao 2017).

When evaluating the use of hydrocolloids in dairy products, rheometry and tribometry are typically applied in conjunction with sensory analysis to evaluate the

M. Baniasadidehkordi · H. S. Joyner (✉)
School of Food Science, University of Idaho, Moscow, ID, USA
e-mail: hjoyner@uidaho.edu

H. S. Joyner (ed.), *Rheology of Semisolid Foods*, Food Engineering Series,
https://doi.org/10.1007/978-3-030-27134-3_12

impact of the hydrocolloids on food texture attributes (Janssen et al. 2007; Sonne et al. 2014; Morell et al. 2016). However, the specific hydrocolloid selected as a fat replacer in dairy products may affect texture not only through its functional properties, but also through hydrocolloid–saliva interactions. Thus, human whole saliva (HWS) has been incorporated during rheological and tribological measurements in multiple studies because of its important role in food texture perception (Guinard et al. 1997). During the initial stages of oral processing, rheological properties are the dominant influence on oral behaviors because they are related to the deformation and change in particle size of foods due to the mastication. After the food is mixed with HWS, broken into small pieces, and formed into a bolus (a mix of food and HWS) in the later stages of oral processing, food tribological behaviors become more important than rheological behaviors. The importance of food tribological behaviors continues with swallowing the food and sensing the remaining food residue on the tongue and palate (Stokes et al. 2013). Because different textural attributes may be perceived during different stages of oral processing, correlating rheological, tribological, and sensory behaviors along with incorporation of HWS during instrumental evaluation of food products can provide a more accurate indication of semisolid food texture attributes for targeted design of nutrient-dense foods that have textures as close as possible to their full-fat counterparts. Thus, the objective of this study was to determine the effects of HWS on the relationships among yogurt microstructures, functionalities, and textures.

2 Materials and Methods

2.1 Materials

Skim milk was purchased from a local supermarket (WinCo Foods, Moscow, ID, USA). Whey protein isolate (WPI) (Provon 190, 89.4% protein) was donated by Glanbia Nutritionals (Fitchburg, WI, USA). Low heat skim milk powder (SMP) and heavy cream (Darigold, 40% fat) were provided by the WSU Creamery (Pullman, WA, USA). Corn starch (CS) and modified potato starch (PS) were donated by Ingredion (Bridgewater, NJ, USA). Locust bean gum (LBG) and carboxymethyl cellulose (CMC) (pre-hydrated Ticalose CMC 2500 powder) were donated by TIC Gums (TIC Gums, Inc., Belcamp, MD, USA). Glucono-delta-lactone (GDL) was donated by Jungbunzlauer (Jungbunzlauer, Inc., MA, USA). The protein assay kit (Quick Start Bradford) used for measuring the protein concentration of HWS was obtained from Bio-Rad laboratories (Bio-Rad laboratories, Inc., CA, USA). Teflon balls (6 mm) for tribometry were purchased from McMaster-Carr (Atlanta, GA, USA). GluconoFluorescein Isothiocyanate (FITC) dye and cavity slides for confocal imaging were purchased from Sigma (Sigma-Aldrich, St. Louis, MO, USA), and Nile red dye was purchased from TCI America (Portland, OR, USA).

2.2 Yogurt Preparation

Twelve yogurts were prepared using skim milk (89.15–97.2% w/w), SMP (0–2.8% w/w), cream (0–3.5% w/w), WPI (0–2.8% w/w), and hydrocolloids, including corn starch (0–1% w/w), potato starch (0–0.7% w/w), LBG (0–1.8% w/w), and CMC (0–1% w/w) (Table 1). These yogurts were selected from 24 previously-studied formulations of acid milk gels based on their significant differences in rheological and tribological properties (Chaps. 10 and 11). Dry powders and cream were added to the skim milk at room temperature (22 ± 2 °C). To disperse the powders, the mixture was stirred with a spatula for 3 min in a water bath (Precision, Thermo Fisher Scientific, Waltham, MA, USA) at 85 °C. Samples were held at 85 °C for 30 min to both ensure pasteurization and complete hydrocolloid dissolution. Samples were then homogenized at 5000 rpm for 1 min using a stand homogenizer (Polytron, Kinematica AG, NY, USA). GDL (1.1–1.55% w/w, see Table 1) was added to samples after cooling to 42.2 °C on the benchtop. Samples were then incubated at 42.2 °C for 4–6 h to reach a pH of 4.55–4.6. The gel was broken with a metal laboratory spatula, then the samples were stored in a refrigerator at 4 °C overnight. Yogurts were blended at 350 rpm for 10 s before testing. Each sample was made in duplicate, and samples were tested the day after preparation.

2.3 Proximate Analyses

All proximate analyses were performed in duplicate. Protein contents were determined with a Leco FP-528 nitrogen analyzer (Leco Corp., St. Joseph, MI, USA) according to the manufacturer's instructions (Kjeldahl conversion factor = 6.38).

Table 1 Experimental design for yogurts

Formula number	SMP (w/w)	Sweet WPI (w/w)	LBG (w/w)	CMC (w/w)	Potato starch (w/w)	Corn starch (w/w)	Skim milk (w/w)	Cream (w/w)	Starter culture (w/w)
1	2.8	0	0	0	0	0	97.2	0	0.04
2	2.83	0	0	0	0	0	95.96	1.21	0.04
3	2.89	0	0	0	0	0	92.26	4.85	0.04
4	2.95	0	0	0	0	0	89.15	7.9	0.04
5	1.8	1	0	0	0	0	97.2	0	0.04
6	1.8	0	1	0	0	0	97.2	0	0.04
7	1.8	0	0	1	0	0	97.2	0	0.04
8	2.1	0	0	0	0.7	0	97.2	0	0.04
9	2.1	0	0	0	0	0.7	97.2	0	0.04
10	0	2.8	0	0	0	0	97.2	0	0.04
11	0	0	1.8	0	0	1	97.2	0	0.04
12	0.2	0.8	0.45	0.45	0.45	0.45	97.2	0	0.04

Fat contents were determined only for samples with added cream using Mojonnier method 989.05 (AOAC 1995a). Moisture contents were determined with a DKN 400 oven (Yamato Scientific America, Inc., Santa Clara, CA, USA), according to the method of the AOAC (1999). Ash contents were determined by using the method from AOAC (1995b) based on dry basis weight. Carbohydrate contents were determined by difference.

2.4 HWS Collection

HWS collection procedure were approved by the University of Idaho Institutional Review Board (protocol 17–196). HWS was collected from five healthy people (three females and two males, ages 20–35) with normal saliva flow according to the method of Bongaerts et al. (2007). Panelists were asked to refrain from eating and drinking anything except water for 2 h prior to collection. At the beginning of collection, they were required to rinse their mouth twice with deionized water and expectorate into a waste cup. They were then asked to chew on the bulb-shaped end of a disposable plastic pipette to stimulate saliva flow and expectorate into a 2 oz. cup. Fresh HWS was collected every 2 h and used for both rheological and tribological testing within 2 h of collection for testing.

2.5 Rheometry

Yogurt rheological behaviors were measured with an Anton Paar MCR 302 rheometer (Anton Paar, Graz, Austria) using a 50 mm diameter parallel plate with a gap height of 1 mm. All tests were carried out at 25 and 8 °C with and without addition of HWS (collected per Sect. 2.4). Samples were equilibrated at the testing temperature for 60 s prior to the test, and all samples were evaluated in triplicate. Shear rate sweeps (0.01–100 s^{-1}) were carried out to measure yogurt viscosity profiles. Oscillatory tests including strain sweeps (0.01–100%, 1 Hz) and frequency sweeps (0.1–100 rad s^{-1} and 0.75% strain) were performed to measure yogurt viscoelastic behaviors. Frequency sweeps were performed at 75% of the lowest critical strain to ensure samples remained in the linear viscoelastic region (LVR). Critical strain was calculated by determining the strain at which G^* deviated by >1% for this study.

2.6 PDMS Plate Production

Polydimethylsiloxane (PDMS) plates were manufactured for tribometry using the method reported by Bongaerts et al. (2007). A curing agent and a base (Dow Corning Corporation, Midland, MI, USA) were used to prepare the plates. The mixture was

poured into an aluminum mold (4 mm height, 60 mm diameter). Air bubbles were removed by a cabinet vacuum desiccator (Bel-Art Products, Wayne, NJ, USA) under a pressure of −90 kPag. Vacuum was applied cyclically up to 10 times until all bubbles were removed. PDMS plates were cured in the mold at 55 °C for 2 h in a DKN 400 oven (Yamato Scientific America, Inc., Santa Clara, CA, USA), then stored overnight at room temperature (22 ± 2 °C) to complete curing. The plates were removed and stored at room temperature (22 ± 2 °C) until used for testing.

2.7 Tribometry

Tribometry was performed using an Anton Paar MCR 302 (Anton Paar, Graz., Austria) with a three-ball (Teflon, 6 mm diameter) geometry on a 60-mm diameter PDMS plate. The materials of the plate and balls were selected to mimic the oral surfaces (tongue–palate) (Johnson et al. 1993; Prakash et al. 2013). A 1 N normal force used was used to mimic the in-mouth force during swallowing, which is between 0.01 and 10 N (Miller and Watkin 1996). The PDMS plate was placed on top of the rheometer base plate and pressed firmly to adhere the two surfaces. A line was marked on both the PDMS plate and rheometer plate using an indelible laboratory pen to provide a visual indicator that the PDMS plate did not move during testing. Friction coefficient was measured at sliding speeds of 0.01–1000 mm s^{-1}. Samples were tested at 25 °C with and without addition of HWS. For samples tested with HWS, 0.5 mL of HWS was added to 3 g of sample and held at room temperature (22 ± 2 °C) for 5 min for complete digestion (Joyner (Melito) et al. 2014). At least three replicates for each sample duplicate were performed with and without HWS. The PDMS plate was cleaned after each run with 70% ethanol and laboratory wipes for non-fat samples; 70% ethyl ether was used for cleaning the surfaces after testing the samples with fat to prevent fat film buildup on the surface of PDMS plates and balls, followed by a rinse with 70% ethanol. Plates and balls were changed after every 6 runs to prevent wear of the tribo-surfaces from impacting the results.

2.8 Textural Evaluation of Yogurts

Sensory evaluation of yogurts was performed with the approval of the University of Idaho's IRB (protocol 17–195). Panelists (n = 10) were recruited from Washington State University (20 min away) and University of Idaho by email and social media. Participants (100% female; ages 25–55 years, mean age of 34 years) were trained for 11 h before evaluating all samples in two sessions. Total training and evaluation of samples was completed over 2 months. Textural attributes (n = 13) were introduced to the participants for describing the texture of the yogurts (Table 2); texture attributes and reference samples were selected from previous related studies (Saint-Eve et al. 2004; Pascua et al. 2013). During training, panelists profiled each yogurt

Table 2 Texture attributes and reference products used for sensory evaluation of yogurts (Saint-Eve et al. 2004; Pascua et al. 2013)

Attribute	Definition	Reference (scale 0–15)
Visual terms		
Lumpiness	Presence of lumps observed in yogurts after being stirred	Yoplait vanilla yogurt = 1 Jell-O tapioca pudding = 15
Spoon viscosity	Thickness of food after being stirred back and forth for 10 times	Water = 1 Jell-O pudding = 10.5
Mouthfeel terms		
Grainy	Feeling of small particles on the tongue after food is swallowed or expectorated	Reddi Wip whipped cream = 1 Gerber baby rice cereal = 12
Mouthcoating	Force required to clear sample adhered to the mouth/with the tongue during eating	Philadelphia cream cheese = 10 Reddi Wip whipped cream = 1
Mouth viscosity	Force needed to draw food from a spoon over the tongue	Water = 1 Jell-O chocolate pudding = 12
Firmness	Firmness of food in the mouth when food is compressed against the palate via tongue motions	Reddi Wip whipped cream = 1 Philadelphia cream cheese = 14
Lumpiness in-mouth	Feeling of lumps in the mouth during eating	Yoplait yogurt = 1 Jell-O tapioca pudding = 15
Smooth	Lack of individual food particles, opposite of grainy and lumpy attributes	Yoplait yogurt = 13 Gerber baby rice cereal = 15
Low-melting	Food does not spread out quickly in the mouth during eating	Reddi Wip whipped cream = 1 Jell-O chocolate pudding = 10
Grittiness	Feeling of gritty/chalky particles in the oral cavity during eating	WalMart non-fat Greek yogurt = 10 Reddi Wip whipped cream = 1
After-feel mouth terms		
Astringent	Astringent/dry sensation in the mouth after food is swallowed or expectorated	Atkins strawberry protein drink = 10 Reddi Wip whipped cream = 1
Chalky/Gritty after-feel	Feeling of chalk-like particles in the mouth after food is swallowed or expectorated	WalMart non-fat Greek yogurt = 10 Reddi Wip whipped cream = 1
Slimy	Difficulty of clearing the mouth from food in the mouth after food is swallowed or expectorated of clearing	Gerber banana baby food = 7 Reddi Wip whipped cream = 1

individually using a 15 cm line scale to indicate the intensity of each attribute present in the samples. Hard copies of descriptions of the 13 attributes along with a 15 cm line scale for each attribute were provided for each training session. Panelists were allowed to practice with the sensory data collection software (Compusense Cloud, Guelph, Ontario, Canada) for the last two training sessions to familiarize themselves with the software for the formal evaluations. Formal sensory evaluation of the 12 yogurt samples was performed in duplicate in separated sensory booths under white light. Samples were coded with 3-digit numbers and evaluated at 8 °C within 48 h of preparation. Six samples were evaluated in duplicate per session. 4 oz. plastic soufflé cups were used for serving the samples. Panelists were asked to rinse their mouths with filtered water, expectorate the samples after each evaluation, and cleanse their palates with unsalted crackers after evaluation of each sample to prevent fatigue. After evaluation of six samples, a 5 min break was required to minimize fatigue and errors. Attribute intensity was marked using a 15 cm line scale with anchors at 1.5 cm for low intensity and 13.5 cm for high intensity. Attribute data were collected from Compusense software for further analysis.

2.9 Confocal Imaging

Confocal laser scanning microscopy (CLSM) was used to image yogurt microstructures. GluconoFluorescein isothiocyanate (FITC) and Nile red dyes were applied to stain yogurt proteins and fat globules, respectively. 8 mg of FITC was added to 500 μL of ethanol in a 1 mL vial and vortexed for 10 s. 500 μL of deionized water was then applied to the FITC solution and vortexed for another 10 s. Nile red solution was prepared similarly, except 5 mg of Nile red was used. FITC and Nile red were used for samples with fat, but only FITC was used for the non-fat samples. Concentrations were adjusted for 120 g yogurt samples. Dyes were added to the yogurt mix before incubation. Samples were incubated, stirred, and stored as described in Sect. 3.2; microscopy analysis was done the next day. For testing, 500 μL of each sample was transferred to a cavity slide and covered with a glass coverslip. Samples were imaged at 20× and 4–8 °C. The wavelengths of Nile red and FITC were excited at 488 nm and 559 nm, respectively.

2.10 Data Analyses

Statistical analyses were performed using SAS version 9.1 (SAS, Cary, NC, USA) and XLSTAT (version 16.11; Addinsoft, Boston, MA, USA). Rheological and tribological graphs were plotted with Origin 8 software (OriginLab, Northampton, MA, USA). Error bars on graphs represent standard deviations of duplicate samples (6 data points total). Viscosity profiles were fitted to four models: Cross-Williams

(Eq. 1), Cross (Eq. 2), Herschel-Bulkley (Eq. 3), and power law (Eq. 4) using TRIOS software version 4.4.0 (TA Instruments; New Castle, DE, USA).

$$\eta = \frac{\eta_o}{\left[1+\left(c\dot{\gamma}\right)^{1-n}\right]} \tag{1}$$

$$\eta = \eta_\infty + \frac{\eta_o - \eta_\infty}{1+\left(k\dot{\gamma}\right)^{n}} k\dot{\gamma}^{n-1} \tag{2}$$

$$\sigma = \sigma_o + k\dot{\gamma}^{n} \tag{3}$$

$$\sigma = k\dot{\gamma}^{n-1} \tag{4}$$

In all equations, η is apparent viscosity (Pa.s) and $\dot{\gamma}$ is shear rate (s^{-1}). In Eq. (1), η_o is the zero-shear rate viscosity (Pa.s), c is the time constant (s), and n is the flow behavior index (unitless). In Eq. (2) η_o is the zero-shear rate viscosity (Pa.s), η_∞ is infinite shear rate viscosity (Pa.s), c is the time constant (s), and n is flow behavior index (unitless). In Eq. (3), σ_o is the yield stress (Pa), k is the consistency coefficient ($Pa.s^{1-n}$) and n is the flow behavior index (unitless). In Eq. (4), k is the consistency coefficient ($Pa.s^{1-n}$) and n (unitless) is the flow behavior index. Friction coefficients between 1 and 100 mm s^{-1} sliding speeds were selected for correlation analysis to mimic oral sliding speed (Malone et al. 2003). These values were used for correlation analysis between tribological–sensory and tribological–rheological results.

ANOVA was used to determine significant differences in sensory results considering three main variables (panelists, replicates, and samples), as well as significant differences among yogurt proximate analysis results and rheological and tribological parameters. Tukey's HSD (Honest Significant Difference) test was used for mean separations. Principal Component Analysis (PCA) was used to determine drivers behind variation of yogurt sensory attributes. Partial Least Square (PLS) analysis was performed to correlate rheological–tribological, rheological–sensory and tribological–sensory results.

3 Results and Discussion

3.1 Formulation Effects on Yogurt Proximate Composition

Significant differences were observed for yogurt protein contents (Table 3). Differences in protein content were attributed to the reduction of SMP for adjustment of other ingredients in the formulation. Sample 11 (added LBG and CS) had the lowest amount of protein, as expected since no SMP powder was added to this formulation. Sample 10 (high WPI level) had the highest protein concentration due

to the use of WPI as the only hydrocolloid. There were also significant differences in moisture content among the samples. Yogurts with higher amounts of hydrocolloids may have retained more water in their microstructure and reduced the availability of the surface water for evaporation. The amount of carbohydrate increased by increasing CS, PS, CMC, and LBG, and decreased with addition of fat and protein, mainly WPI, which was expected. This effect was observed in samples 12 (all hydrocolloids added) and 9 (added CS), which had the highest carbohydrate content, and samples 4 (full-fat) and 10 (high WPI level), which had the lowest carbohydrate content. There were no significant differences in yogurt ash contents, which was not surprising considering the bulk of the minerals in yogurt are from the milk, not the texture-modifying ingredients.

3.2 Formualtion and HWS Effects on Yogurt Microstructures

Overall, CLSM results showed the conformation of protein network microstructure (green) was dependent on yogurt formulation, and the size of serum pores increased with addition of hydrocolloids (black areas in Figs. 1, 2, and 3). Pores size in samples with gums (samples 6, 7, and 12, Fig. 2d, g; 3g) were significantly bigger than those in the control sample (sample 1, Fig. 1a). LBG, used in sample 6, is a neutral hydrocolloid, so there would be minimal electrostatic interaction between LBG and caseins at the pI of casein (4.6, close to the pH of all samples, which was ~4.5), causing a weaker network. However, LBG can increase viscosity by increasing the continuous phase viscosity, which would likely result in the smaller, more weakly aggregated protein network in these samples (Perrechil et al. 2009).

Table 3 Yogurt proximate compositions[1]

Formula number	Protein (%)	Moisture (%)	Fat (%)	Ash (%)	Carbohydrate (%)[2]
1	5.61 ± 0.075^{bc}	85.12 ± 0.092^{abc}	0	0.78 ± 0.028^{a}	8.8^{abc}
2	5.36 ± 0.249^{dc}	83.54 ± 0.922^{c}	0.50 ± 0.022^{a}	0.65 ± 0.006^{a}	9.9^{ab}
3	4.64 ± 0.129^{efg}	86.00 ± 0.406^{a}	1.98 ± 0.008^{b}	0.70 ± 0.048^{a}	7.26^{de}
4	4.62 ± 0.006^{fg}	85.01 ± 0.496^{abc}	3.52 ± 0.142^{c}	0.62 ± 0.008^{a}	6.99^{e}
5	6.07 ± 0.094^{b}	85.86 ± 0.132^{abc}	0	0.79 ± 0.017^{a}	7.90^{dc}
6	4.65 ± 0.015^{efg}	86.61 ± 0.207^{a}	0	0.69 ± 0.003^{a}	8.77^{bc}
7	4.56 ± 0.075^{fg}	85.21 ± 0.084^{abc}	0	0.74 ± 0.09^{a}	9.73^{ab}
8	5.04 ± 0.053^{de}	85.68 ± 0.394^{ab}	0	0.70 ± 0.024^{a}	9.1^{abc}
9	4.82 ± 0.035^{efg}	85.06 ± 0.612^{bc}	0	0.76 ± 0.069^{a}	9.45^{a}
10	6.79 ± 0.153^{a}	86.07 ± 0.363^{abc}	0	0.73 ± 0.088^{a}	7.06^{de}
11	4.48 ± 0.034^{g}	86.62 ± 0.061^{a}	0	0.67 ± 0.082^{a}	8.83^{abc}
12	4.96 ± 0.024^{def}	84.43 ± 0.162^{bc}	0	0.65 ± 0.025^{a}	10.03^{a}

[1]Different letters in a given column indicate significant differences at $p \leq 0.05$
[2]Carbohydrates were calculated by difference

The greater amount of serum observed in the microscopy images for sample 6 (added LBG, Fig. 2d) was in line with its higher moisture content (Table 3). Also, the moisture content of the sample containing all hydrocolloids (sample 12) was significantly lower than that of samples 6 (added LBG) and 7 (added CMC, Fig. 2g), which may be related to differences in their pores sizes. The protein network in the sample with added CMC (sample 7) was shown to be thicker and more compact than that of the sample with added LBG (sample 6). This was attributed to casein–CMC interactions, which occurred due to the opposite charges on CMC and milk proteins at yogurt pH and resulted in a stronger protein network. The denser protein matrix of sample 5 (Fig. 2a) compared to the control sample (sample 1) was attributed to higher protein content (Table 3). Addition of WPI can increase the level of casein–casein and casein–whey interactions and result in greater cross-linking and a denser microstructure with more protein chains. Addition of fat in samples 2 and

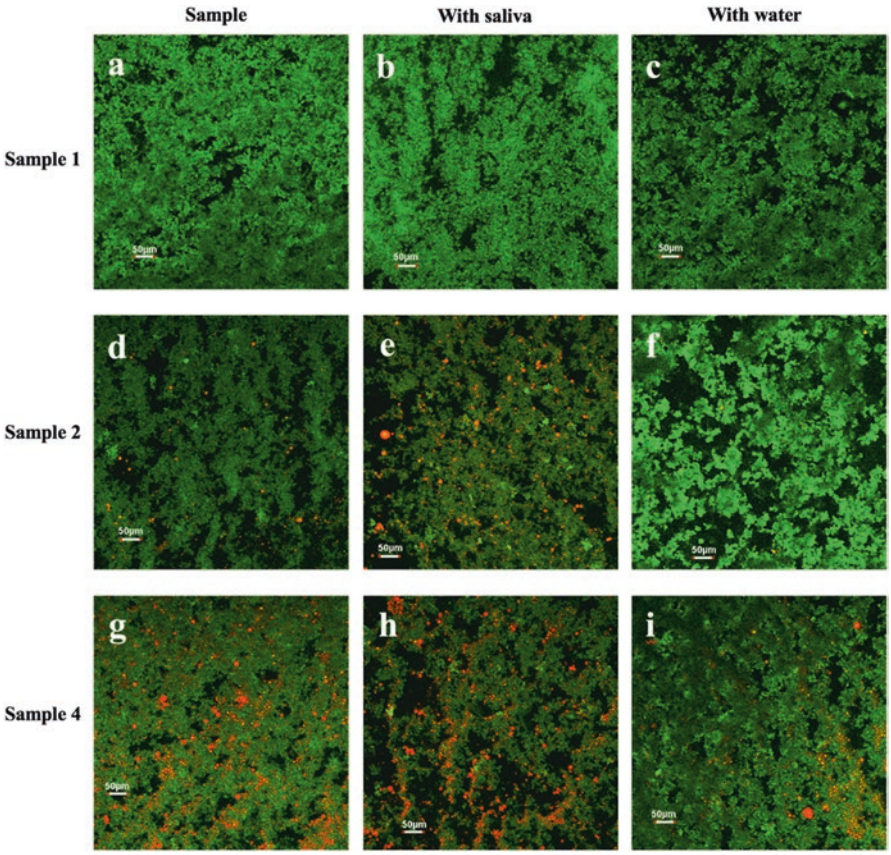

Fig. 1 CLSM results of yogurts; (**a**) sample 1; (**b**) sample 1 with HWS; (**c**) sample 1 with water; (**d**) sample 2; (**e**) sample 2 with HWS; (**f**) sample 2 with water; (**g**) sample 4; (**h**) sample 4 with HWS; (**i**) sample 4 with water. The protein network, fat globules, and serum pores are shown in green, red, and black, respectively

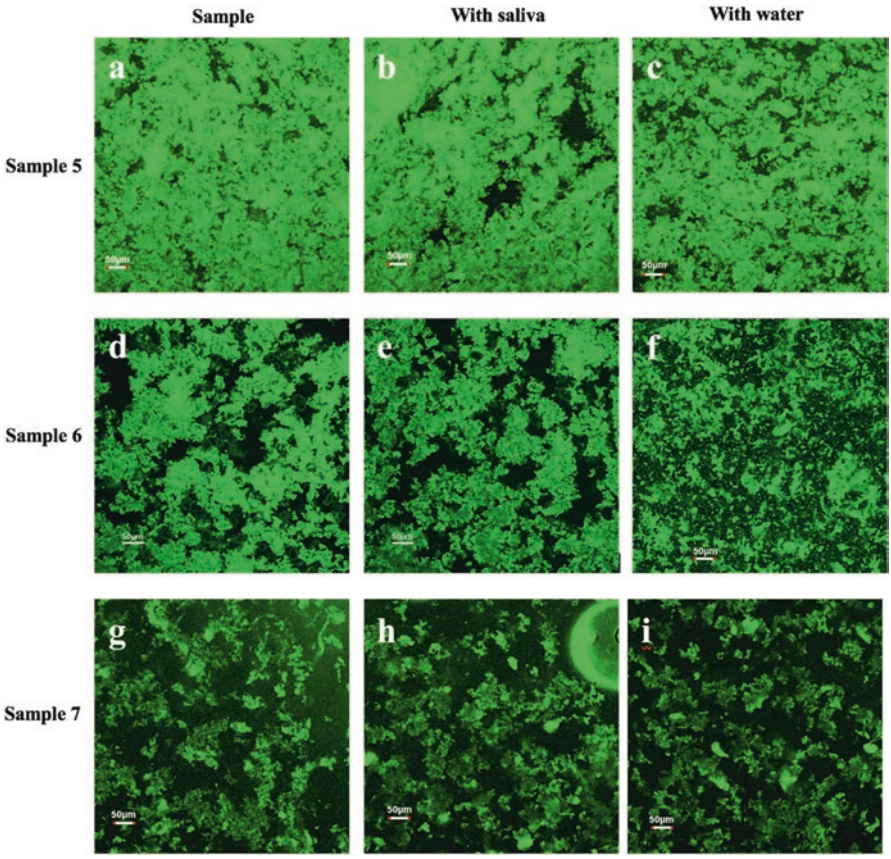

Fig. 2 CLSM results of yogurts; (**a**) sample 5; (**b**) sample 5 with HWS; (**c**) sample 5 with water; (**d**) sample 6; (**e**) sample 6 with HWS; (**f**) sample 6 with water; (**g**) sample 7; (**h**) sample 7 with HWS; (**i**) sample 7 with water. The protein network and serum pores are shown in green and black, respectively

4 caused a denser protein microstructure compared to the control sample (sample 1). This result was in agreement with other studies of microstructural features of yogurts produced by homogenized milk (Serra et al. 2007).

In general, addition of HWS caused greater protein aggregation regardless of formulation. This effect was most clearly illustrated for the control sample (sample 1, Fig. 1b), and samples with added PS (sample 8, Fig. 3b) and CS (sample 9, Fig. 3e) when HWS was added. The greater effect of HWS on the starch-containing samples was likely because amylase breaks down amylose in starch to smaller sugars (Janssen et al. 2007). This would cause disruption of the starch embedded in the casein network and result in a larger serum phase. In addition, HWS caused fat coalescence in samples 2 and 4 (Fig. 1e, h). This observation was attributed to depletion flocculation created by the osmotic pressure from salivary proteins

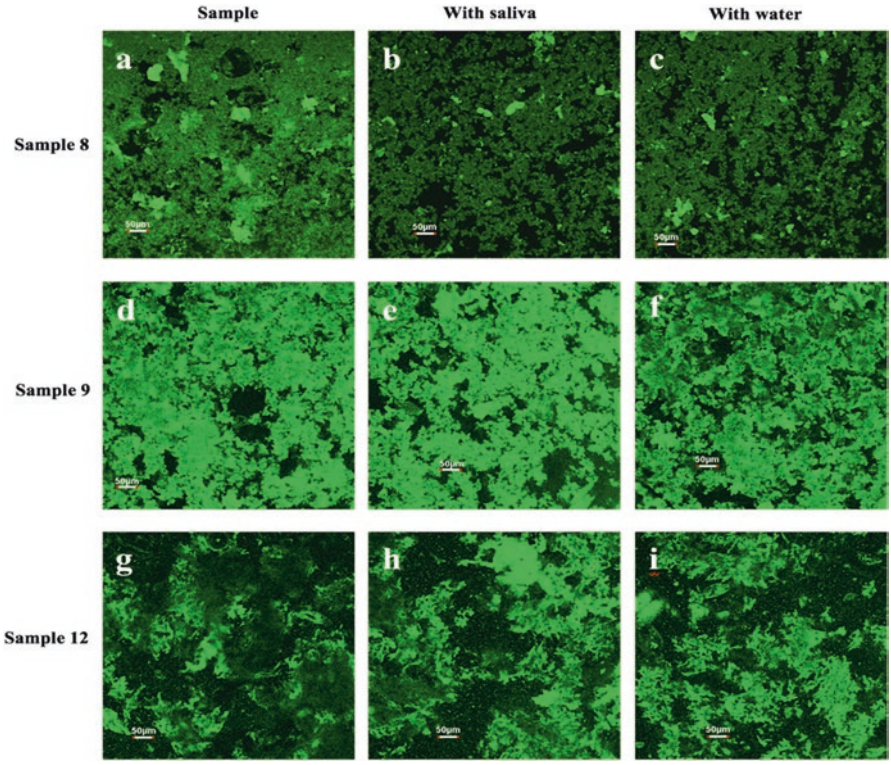

Fig. 3 CLSM results of yogurts; (**a**) sample 8; (**b**) sample 8 with HWS; (**c**) sample 8 with water; (**d**) sample 9; (**e**) sample 9 with HWS; (**f**) sample 9 with water; (**g**) sample 12; (**h**) sample 12 with HWS; (**i**) sample 12 with water. The protein network and serum pores are shown in green and black, respectively

Table 4 Main sources of variation of flow properties of yogurts (n = 12) determined by F-values obtained from three-way ANOVA[a]

Source of variation	η_o (Pa.s)	n	k (Pa.s^{1-n})
Formulations	16.4***	1.2	1.8
HWS	12.5***	1.3	0.4
Temperature	9.7***	1	1.2
HWS × temperature	1.9	1	0.1
Formulation × HWS	6.1**	1	1.2
Formulation × temperature	4.8**	1	0.8

[a]*, **, and *** indicate significant differences at $p \leq 0.05$, $p \leq 0.01$, and $p \leq 0.001$, respectively

(Chen 2015). However, the effect of HWS was not notable on the microstructures of samples prepared with gums (samples 6, 7, and 12, Fig. 2e, h, Fig. 3h), indicating that saliva had little interaction with the gums, as expected.

Overall, addition of HWS had different effects on yogurt microstructures, particularly the protein network, than the effects from the addition of water. Addition of water to the samples notably increased the porosity in all yogurts due to the dilution effect of water and its integration into the serum pores. The dilution effect of water was shown most clearly for the sample containing LBG (sample 6, Fig. 2f). This results was attributed to the weaker microstructure of LBG in the continuous phase due to disrupted weak interactions, e.g. hydrogen and non-covalent bonds, upon addition of water (Murray and Phisarnchananan 2014) compared to the samples with stronger interactions, such as covalent bonds and hydrophobic interactions with casein micelles.

3.3 Formulation and HWS Effects on Yogurt Rheological Behaviors

3.3.1 Yogurt Viscosity Behaviors

Three-way ANOVA was used to determine the effects of formulation (hydrocolloids), HWS, and temperature on the flow parameters from non-Newtonian models of yogurts including η_0, n, and c (Table 4). For η_0, formulation, HWS, and temperature showed significant effects at $p \leq 0.001$, as well as significant effects at $p \leq 0.01$ for the interaction of formulation with each of the other two parameters. Interaction of HWS with temperature for η_0 was not significant. Surprisingly, no significant effects were observed for n or k for any combination of parameters. These results might have been caused by the dominant role of η_0 in the non-Newtonian viscosity models compared to n or k (see subsequent discussion).

The significant impact of hydrocolloids can be mainly explained by (1) the electrostatic interactions between counterions of anionic hydrocolloids with casein micelles, (2) swelling of starch granules in the presence of water and heat in the yogurt system, and (3) dispersion of large, neutral hydrocolloid particles in the continuous phase and their depletion flocculation effects. These factors can also significantly change the microstructure of protein network and overall conformation of yogurts (Figs. 1, 2, and 3). The significant effects from HWS were attributed to the digestive, dissolving, and coalescence properties of HWS resulting mostly from the enzymes, salivary proteins, and electrolytes present in HWS. Temperature can weaken the intermolecular bonds in a semisolid food system, decrease resistance to flow, and lower the viscosity (Berk 2018). Based on these results, the importance of hydrocolloids, HWS, and temperature on yogurt flow properties as a model system for semisolid foods can be helpful in designing semisolid foods with specific rheological properties.

All yogurts showed shear-thinning behavior (Tables 5, 6, 7, and 8). Shear-thinning behavior in a yogurt system is typically due to alignment of entangled protein molecules with the shear field. The viscosity curves of all samples were fit to Cross-Williams, ($R^2 > 0.935$) Cross ($R^2 > 0.748$), Herschel-Bulkley ($R^2 > 0.74$), and power law ($R^2 > 0.985$) models. The best-fit model varied by formulation. Formulations with added fat tended to fit best to the Cross model, while formulations incorporating hydrocolloids tended to fit better to the Herschel-Bulkley and Cross-Williams models. While all the models used for fitting are suitable for shear-thinning materials, there are a few key differences among them. The main difference between the Cross model and the Cross-Williams model is the presence of η_∞ (Pa s) in the Cross model; η_∞ is indicative of shear-independent flow behavior under high-shear conditions. The primary difference between the power law and Herschel-Bulkley models is the yield stress in the Herschel-Bulkley model. The differences in best-fit model results were likely due to the more complex microstructures in samples containing hydrocolloids. The presence of hydrocolloids can result in a yield stress and persistent shear-thinning behavior even at very high shear rates due to polymer entanglements that break down with increasing shear. Without these entanglements, such as in samples 2, 3, and 4 (fat-containing samples with no added gums or starches), there is less structure to break down under shear, resulting in little to no yield stress and a viscosity plateau at higher shear rates.

Generally, η_0, η_∞, n, and σ_o decreased with increasing temperature and addition of HWS. Addition of hydrocolloids increased the viscosity, except for the sample with LBG (sample 6). This sample was also the only one fitted to a power law model, which is mostly applicable to weak gels, although the protein microstructure was shown to be highly entangled (Fig. 2) compared to the control sample (sample 1, Fig. 1). These entanglements have been observed previously (Murray and Phisarnchananan 2014). LBG is a neutral hydrocolloid that increases the viscosity of the system by increasing the continuous phase, not through interactions with protein network (Hansen 1993). Another mechanism for the viscosity increase

Table 5 Viscosity profiles for yogurts ($n = 12$) at 8 °C without added HWS

Formula	Model	η_o (Pa.s)	η_∞ (Pa.s)	n	c (s)	k (Pa.s^{1-n})	σ_0 (Pa)	R^2
1	Herschel-Bulkley	–	–	0.955	–	0.177	14.9	0.740
2	Cross	2190	0.212	0.935	31.2	–	–	0.891
3	Cross	693	0.222	0.930	19.8	–	–	0.895
4	Cross	627	0.214	0.926	19.7	–	–	0.919
5	Cross	532	0.020	0.966	65.5	–	–	0.820
6	Power law	56.1	–	0.286	–	–	–	0.985
7	Cross-Williamson	1358	–	0.928	13.0	–	–	0.935
8	Herschel-Bulkley	–	–	0.902	–	0.157	26.0	0.806
9	Herschel-Bulkley	–	–	0.772	–	0.682	19.5	0.856
10	Cross	13,476	0.02	0.971	19.5	–	–	0.748
11	Cross-Williamson	370	–	0.697	8.80	–	–	0.999
12	Cross-Williamson	416	–	0.834	10.33	–	–	1.000

Table 6 Viscosity profiles for yogurts (n = 12) at 8 °C with added HWS

Formula	Model	η_o (Pa.s)	η_∞ (Pa.s)	n	c (s)	k (Pa.s^{1-n})	σ_0 (Pa)	R^2
1	Cross-Williamson	254	–	0.891512	64	–	–	0.999
2	Cross	637	0.101	0.914	25.5	–	–	0.938
3	Cross	418	0.122	0.908	28.2	–	–	0.965
4	Cross	531	0.174	0.911	37.8	–	–	0.922
5	Cross	461	0.010	0.949	52.1	–	–	0.917
6	Power law	29.3	–	0.324	–	–	–	0.992
7	Cross-Williamson	232	–	0.805	11.3	–	–	1.000
8	Herschel-Bulkley	–	–	0.746	–	0.176	6.61	0.975
9	Herschel-Bulkley	–	–	0.387	–	3.05	5.71	0.962
10	Cross	3976	0.09	0.961	34.5	–	–	0.961
11	Cross-Williamson	184	–	0.699	5.13	–	–	0.999
12	Cross-Williamson	141	–	0.755	11.3	–	–	1.000

Table 7 Viscosity profiles for yogurts (n = 12) at 25 °C without added HWS

Formula	Model	η_o (Pa.s)	η_∞ (Pa.s)	n	c (s)	k (Pa.s^{1-n})	σ_0 (Pa)	R^2
1	Herschel-Bulkley	–	–	0.856	–	0.199	7.39	0.871
2	Cross	1177	0.054	0.928	19.9	–	–	0.881
3	Cross	364	0.109	0.920	22.6	–	–	0.924
4	Cross	344	0.086	11.6	0.916	–	–	0.948
5	Cross	471	0.013	0.957	55.8	–	–	0.952
6	Power law	29.5	–	0.358	–	–	–	0.993
7	Cross-Williamson	454	–	0.825	12.6	–	–	0.998
8	Herschel-Bulkley	–	–	0.776	–	0.289	15.3	0.924
9	Herschel-Bulkley	–	–	0.841	–	0.322	11.0	0.880
10	Cross	4712	0.01	0.957	79.691	–	–	0.970
11	Cross-Williamson	223	–	0.649	7.49	–	–	0.999
12	Cross-Williamson	219	–	0.776	10.6	–	–	1.000

observed for neutral hydrocolloids is depletion flocculation. The large LBG molecules would create an increased osmotic pressure between the casein micelles, which would push the caseins together and cause flocculation (Thaiudom and Goff 2003). Samples with LBG (sample 6) and LBG and CS (sample 11) also showed the least decrease in their viscosity upon addition of HWS, which was expected based on the confocal images (Fig. 2). Similar results were shown with LBG solutions and HWS (Zinoviadou et al. 2008).

The viscosity of sample 11 slightly increased compared to the control due to inclusion of LBG and CS, which was expected because addition of CS and LBG together in a system can make a stronger gel than when LBG is used individually (Murray and Phisarnchananan 2014). The viscosity of sample 7 increased notably from the control due to addition of CMC. CMC is an anionic gum that interacts with

Table 12.8 Viscosity profiles for yogurts (n = 12) at 25 °C with added HWS

Formula	Model	η_o (Pa.s)	η_∞ (Pa.s)	n	c (s)	k (Pa.s^{1-n})	σ_0 (Pa)	R^2
1	Cross-Williamson	84.4	–	1	19.2	–	–	0.999
2	Cross	305	0.047	0.910	23.7	–	–	0.964
3	Cross	226	0.061	0.907	26.5	–	–	0.975
4	Cross	345	0.083	0.909	33.2	–	–	0.943
5	Cross-Williamson	214	–	0.946	33.1	–	–	0.900
6	Power law	15.5	–	0.391	–	–	–	0.996
7	Cross-Williamson	106	–	0.755	10.6	–	–	1.000
8	Herschel-Bulkley	–	–	0.601	–	0.272	4.89	0.954
9	Herschel-Bulkley	–	–	0.532	–	0.830	3.69	0.961
10	Cross	648	0.01	0.908	11.5	–	–	0.760
11	Cross-Williamson	106	–	0.624	6.96	–	–	0.999
12	Cross-Williamson	79.9	–	0.693	13.7	–	–	1.000

positively charged casein micelles through aggregative phase separation to create a strong matrix (van de Velde et al. 2015). The yield stress of sample 8, which contained PS, was higher than that of sample 9, which contained CS. PS can increase viscosity due to the large size of its swollen starch granules in the dispersed phase. CS is a neutral polysaccharide that can increase viscosity through weak interactions in the continuous phase (Dang et al. 2009). The network formed by CS and milk protein is not as strong as the PS–milk protein network; hence, the force (σ_o) that was needed for sample 8 (added PS) to flow was greater than that for sample 9 (added CS) due to the increased size of the starch granules.

Sample 10, which incorporated WPI, had the highest viscosity of all samples, likely because of its high protein content (Table 2). Denaturation of whey proteins occurs due to heat treatment above 70 °C. High concentration of denatured whey proteins results not only in increased interactions with casein micelles but also in interactions among non-associated whey proteins. These interactions yield a stronger protein gel network with more cross-linking and a more aggregate microstructure (Lucey and Singh 1997). Sample 5, which also contained WPI but at a lower concentration, showed similar results, although its viscosity was lower than sample 10 likely due to its lower protein content (Table 2). Interestingly, the viscosity of sample 12 was not similar to that of the other samples even though it contained all hydrocolloids. This result was attributed to the conflicting contributions of hydrocolloids in this sample.

Addition of fat notably increased viscosity (samples 2, 3, and 4), likely due to the embedded fat globules throughout the protein matrix creating a resistance to flow (Chojnicka-Paszun et al. 2012; Nguyen et al. 2017). Full-fat yogurt (sample 4) showed higher viscosity than samples 2 and 3, supporting this hypothesis.

Yogurt viscosity and n values decreased with addition of HWS and increased temperature (Tables 5, 6, 7, and 8). Samples evaluated with added HWS at 25 °C showed the lowest viscosity (Table 8), which was expected. Increasing temperature weakens the intermolecular bonds in a yogurt system, decreasing resistance to flow

and lowering the viscosity (Berk 2018). The effect of HWS varied based on the type(s) of hydrocolloids used in the formulations. Salivary proteins, enzymes, and other HWS components can disrupt semisolid food microstructures (Janssen et al. 2007). For example, HWS has been shown to cause protein flocculation when mixed with yogurt (Vingerhoeds et al. 2009; Sarkar and Singh 2012). These effects can be observed in the microstructural images (Figs. 1, 2, and 3). Samples containing PS (sample 8) and CS (sample 9) showed the greatest decrease in yield stress upon addition of HWS. Similar results were reported for starch-based custards (Janssen et al. 2007). Amylase in the HWS would break down the amylose in the starches into simple sugars like maltose and glucose (Humphrey and Williamson 2001). Although this effect was not clearly observed in the confocal images of sample 8 (added PS) in this study, the digestion of PS by amylase was visually shown by another study (Janssen et al. 2007).

3.3.2 Yogurt Viscoelastic Behaviors

The effects of formulation (hydrocolloids), HWS, and temperature on yogurt viscoelastic properties, including critical strain (γ_c, %), G^* (complex modulus at γ_c, Pa), and tan δ (phase angle at γ_c, rad), were determined using F-values from three-way ANOVA (Table 9). Formulation and temperature showed significant effects at $p \leq 0.001$ for tan δ and γ_c.; HWS also showed significant effects on tan δ ($p < 0.001$) and γ_c ($p < 0.01$). Additionally, significance at $p < 0.01$ was observed for the interaction of formulation with temperature on tan δ and γ_c. HWS was the only parameter that had a significant effect on G^* ($p \leq 0.05$). However, temperature was borderline for significance ($p \leq 0.07$). This finding might explain the significant differences of G^* values from Tukey's HSD with different temperatures (Table 10). The significant changes in G^* may have been due to the increased stability and resistance to permanent deformation observed in yogurts with added hydrocolloids compared to the control sample. For example, starches (PS and CS) and gums (CMC and LBG) can improve gel stability by increasing the number of internal molecular interactions as well as by creating stronger bonds through different mechanisms. HWS effects were also likely due to structural changes upon its addition. As previously

Table 9 F-values for sources of variation of viscoelastic properties of yogurts ($n = 12$) obtained from three-way ANOVA[a]

Source of variation	γ_c	G^*	tan δ
Formulations	45***	2.5	418***
HWS	10.8**	4.6*	121***
Temperature	75.1***	4	72.4***
HWS × temperature	1.5	1.8	0.4
Formulation × HWS	2.3	1.2	38.7***
Formulation × temperature	5.1**	1.2	4.4**

[1]γ_c. critical strain, G^*: complex modulus at γ_c, tan δ: phase angle at γ_c

[a]*, **, and *** indicate significant differences at $p \leq 0.05$, $p \leq 0.01$, and $p \leq 0.001$, respectively

Table 10 Viscoelastic parameters of 12 yogurts measured by strain sweep at 1 Hz[1]

Formula number	γ_c (%) 8 °C NS	γ_c (%) 8 °C S	γ_c (%) 25 °C NS	γ_c (%) 25 °C S	G^* (Pa) 8 °C NS	G^* (Pa) 8 °C S	G^* (Pa) 25 °C NS	G^* (Pa) 25 °C S	tan δ (rad) 8 °C NS	tan δ (rad) 8 °C S	tan δ (rad) 25 °C NS	tan δ (rad) 25 °C S
1	1.74^{a}	1.30^{a}	3.12^{a}	2.33^{a}	66.2^{e}	43.6^{h}	56.4^{e}	33.2^{f}	0.313^{cd}	0.345^{e}	0.3475^{e}	0.355^{d}
2	0.731^{d}	0.976^{b}	1.74^{b}	1.30^{b}	448^{b}	249^{c}	178^{c}	171^{c}	0.298^{cde}	0.317^{fg}	0.336^{cd}	0.334^{g}
3	0.411^{f}	0.547^{e}	0.731^{e}	0.730^{e}	230^{d}	103^{gf}	133^{d}	63.8^{e}	0.296^{cdef}	0.320^{f}	0.320^{de}	0.336^{fg}
4	0.731^{d}	0.411^{f}	0.547^{f}	0.730^{e}	323^{bcd}	133^{e}	168^{c}	67.1^{e}	0.314^{cd}	0.329^{ef}	0.327^{cd}	0.349^{ef}
5	0.548^{e}	0.731^{c}	0.976^{d}	0.976^{c}	415^{b}	278^{b}	245^{b}	205^{b}	0.319^{c}	0.333^{ef}	0.341^{cd}	0.332^{g}
6	0.548^{e}	0.411^{f}	0.547^{f}	0.411^{g}	380^{bc}	206^{d}	187^{c}	102^{d}	0.571^{a}	0.591^{b}	0.665^{a}	0.639^{b}
7	1.30^{b}	0.976^{b}	1.74^{b}	1.30^{b}	257^{cd}	125^{ef}	128^{d}	63.1^{e}	0.502^{b}	0.555^{c}	0.588^{b}	0.626^{bc}
8	0.548^{e}	0.411^{f}	0.976^{d}	0.547^{f}	360^{bcd}	90.0^{g}	231^{b}	39.1^{f}	0.287^{def}	0.340^{e}	0.295^{f}	0.352^{e}
9	0.411^{f}	0.411^{f}	0.411^{g}	0.547^{f}	253^{cd}	122^{ef}	134^{d}	65.8^{e}	0.280^{ef}	0.300^{g}	0.287^{f}	0.3137^{h}
10	0.547^{e}	0.548^{d}	0.976^{d}	0.976^{c}	3410^{a}	516^{a}	499^{a}	329^{a}	0.268^{f}	0.300^{g}	0.298^{ef}	0.301^{h}
11	0.961^{c}	0.731^{c}	1.29^{c}	0.975^{d}	327^{bcd}	198^{d}	245^{b}	115^{d}	0.553^{a}	0.861^{a}	0.595^{b}	0.984^{a}
12	0.411^{f}	0.411^{f}	0.731^{e}	0.730^{e}	347^{bcd}	136^{e}	184^{c}	67.3^{e}	0.502^{b}	0.532^{d}	0.595^{b}	0.621^{c}

[1]γ_c: critical strain, G^*: complex modulus at γ_c, tan δ: phase angle at γ_c
Letters in each column that are different indicate significant differences

discussed, HWS can disrupt semisolid food microstructures through digestion, osmotic pressure, dilution, or net charge alteration. Similarly, increasing temperature allows internal molecules to move more easily and quickly from the additional heat energy, which can decrease molecular bond strength. As a result, the yogurts can lose their original microstructures and become more susceptible to external shear when mechanical force is applied.

Overall, there were significant differences in γ_c, G^*, and tan δ among the 12 yogurt formulations (Table 10). γ_c increased or remained constant with increasing temperature except for sample 4 (full-fat yogurt). The decrease in γ_c value for sample 4 was unexpected but may have been due to increased thermal energy of the oil-in-water emulsion in sample 4 at increased temperature, which would decrease the viscosity of the fat globules, resulting in fat coalescence. The molecules would then deform more easily when shear stress is applied, yielding a smaller γ_c. The increasing γ_c values for the other samples can be explained by thermodynamics. At higher temperatures, molecular mobility increases, resulting in more fluid-like behavior and requiring a greater force to induce nonlinear behavior. Fluids are less likely to show nonlinear viscoelastic behavior at lower strains because nonlinear viscoelastic behavior indicates irreversible structural changes. Since fluids tend to have less complex microstructures, it is more difficult to induce irreversible change to that structure. γ_c values of fat-containing samples (samples 2, 3, and 4) increased with addition of HWS. This could be due to fat flocculation resulting from the osmotic pressure of salivary proteins throughout the sample (Huc et al. 2016), decreasing structural complexity and resulting in more resistance to permanent deformation from applied strain.

HWS had a different impact on critical strain values compared to that of temperature. γ_c decreased for most samples with added hydrocolloids. This result may have been due to the destabilization of the original protein microstructure after incorporation of HWS. HWS has the largest effect on the sample with PS (sample 8) compared to the other yogurt samples. This result was attributed to enzymatic breakdown of the starch granules by the amylase in HWS. However, the changes in the microstructure of semisolid food upon addition of HWS can also be explained by other mechanisms, e.g. depletion flocculation. The non-adsorbing molecules in HWS can create an osmotic pressure that forces the aggregation of the emulsion droplets and results in microstructural disruption (Chen 2015).

Overall, G^* decreased with increasing temperature and HWS addition to the samples. G^* values of samples with added PS (sample 8) drastically decreased with the addition of HWS, but this effect was not shown for samples with CS (sample 9). This result was probably due to the high degree of PS–salivary amylase interactions. A similar effect for samples 8 and 9 was also seen in the shear rate sweep results (Sect. 3.3.1). This result can be explained by the higher amount of amylose in CS (Singh et al. 2003). PS has more highly branched amylopectin and lower amylose content compared to large proportion of linear amylose in CS. Saliva can more easily pass through large, open starch granules than highly compacted microstructures (Bird et al. 2000). As a result, amylose is more difficult to digest compared to highly

branched amylopectin since the linear amyloses can pack tightly because of their shape. This results in less accessible area on high-amylose starch granules for digestion. Additionally, the compact microstructure of CS results in an increase in gelatinization temperature; when gelatinized, a high proportion of amylose in the starch granules promotes rapid retrogradation (Bird et al. 2000; Singh et al. 2003). Retrogradation is the molecular interaction of starch chains via hydrogen bonds when a gelatinized starch paste is cooled (Hoover 2001). This phenomenon results in the formation of small, insoluble amylose crystallites that move to the available spaces between the amylopectin branches and increase resistance to enzymatic digestion (Bird et al. 2000).

tan δ values increased with added HWS and increased temperature, indicating increased viscous-type behavior. Sample 10, containing WPI, showed the lowest tan δ values, and samples containing LBG (samples 6 and 11) had the highest. Sample 11 (added LBG and CS) showed tan $\delta = 0.99$, indicating approximately equal viscous and elastic moduli with added HWS at 25 °C. Addition of CS, PS, or high levels of WPI (samples 9, 8, and 10, respectively) resulted in smaller tan δ values compared to those of the samples containing fat (samples 2, 3, and 4). As expected, the addition of HWS resulted in greater tan δ values for starch-containing samples (samples 8 and 9) due to starch breakdown by salivary α-amylase. tan δ values for the sample with CMC (sample 7) and the sample with all hydrocolloids (sample 12) were similar. These results may have been indicative of the similar matrix conformation of these two samples, which can be observed in the confocal images of these two samples (Figs. 2 and 3).

Frequency sweep results (Fig. 4) showed that formulation had a notable impact on frequency-dependent behavior. Samples with high levels of WPI (sample 10), full-fat samples (sample 4), and added PS (sample 8) had low dependence of frequency as indicated by the small slope of the viscoelastic moduli. These results were attributed to the presence of covalent bonds in the protein matrix for this sample (Laverse et al. 2011). G' values for samples with LBG (sample 6) and LBG and CS (sample 11) showed high frequency dependence. These samples were weak gels with non-covalent linkages such as hydrogen bonds rather than electrostatic bonds (Laverse et al. 2011; Tang and Liu 2013). The weak molecular structure in samples 6 and 11 can be easily disrupted as the frequency increased from 0.1 to 100 rad s^{-1}. This resulted in an increased slope compared to samples 4, 8, and 10. Another notable difference among formulations was the gap between G' and G''. Samples 4, 8, and 10 had a greater gap between the two moduli, indicating a stronger microstructure compared to samples with a smaller gap between G' and G'', such as samples 6 and 11. The weaker microstructure in samples 6 and 11 was likely caused by destabilization of protein network caused by dispersion of neutral LBG molecules in the continuous phase and depletion flocculation resulting from the altered osmotic pressure within the protein network. Furthermore, it has been shown that a combination of LBG and milk proteins can result in a weak gel due to the thermodynamic incompatibility of LBG (Thaiudom and Goff 2003).

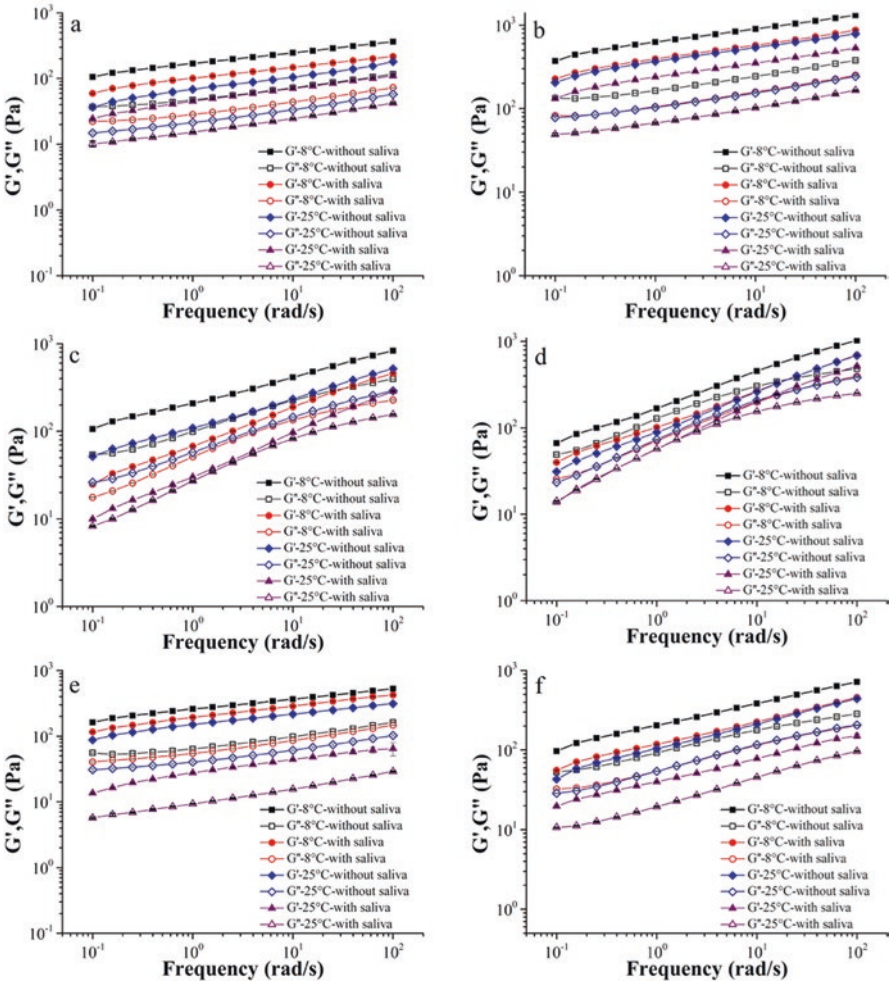

Fig. 4 Frequency sweep results of yogurts; (**a**) sample 4; (**b**) sample 10; (**c**) sample 6; (**d**) sample 11; (**e**) sample 8; (**f**) sample 12

3.4 Effect of Formulation and HWS on Yogurt Friction Profiles

Three-way ANOVA was performed to determine the impact of formulation (hydrocolloids), HWS, and different rates of sliding speeds on yogurt friction coefficients (Table 11). A range of sliding speeds between 10 and 100 mm s^{-1} were selected to mimic oral sliding speeds experienced during consumption of yogurts and other semisolid products (Malone et al. 2003). The effects of formulation, sliding speed, and the interaction of formulation with the other two parameters were all significant

Table 11 Effect of main sources of variation of frictional properties of yogurts ($n = 12$) determined by F-values obtained from three-way ANOVA[a]

Source of variations	Friction coefficient
Formulation	377***
Sliding speed	26.6***
HWS	710*
Sliding speed × HWS	6.6**
Formulation × HWS	131***
Formulation × sliding speed	2.8***

[a]*, **, and *** indicate significant differences at $p \leq 0.05$, $p \leq 0.01$, and $p \leq 0.001$, respectively

at $p \leq 0.001$. HWS was significant at $p \leq 0.05$, and the interaction of sliding speed with HWS was significant at $p \leq 0.01$. Salivary proteins, mainly high molecular weight and proline-rich proteins, e.g. mucins, are the main source for the high lubricity of HWS (Bongaerts et al. 2007). HWS has been shown to have friction coefficients that were two orders of magnitude lower than those of water in its boundary regime. The significant impact of formulation was likely due to the addition of hydrocolloids with significantly different functionalities due to their different electrostatic charges, molecular size, and adhesive properties. This can result in significantly different network microstructures, number of intermolecular interactions, bond strength, and aggregate size, all of which can dramatically alter the frictional behaviors of the yogurt formulations. For instance, addition of WPI can lead to a larger particle size that can increase friction coefficients. Additionally, sliding speed can change the position of food between the two surfaces (balls and PDMS plate) and impact the friction coefficient.

Stribeck curves for the yogurt samples showed an increase in friction coefficient at the beginning of the curve up to approximately 0.1 mm s^{-1} (Fig. 5). This increase was not a hydrodynamic regime, but was due to elastic deformation of the PDMS plate because the rotational speed of the double-ball attachment was not high enough to allow slip (Zinoviadou et al. 2008). This start-up behavior typically disappeared at a sliding speed of ~0.1 mm s^{-1} and was minimal in full-fat yogurt (sample 4). During testing, fat globules form an interfacial film between the sliding surfaces, acting as a lubricant and resulting in a notable decrease in friction coefficient, which would promote sliding rather than stretching of the PDMS plate (Prakash et al. 2013; Huc et al. 2016).

The profile shape of Stribeck curves significantly changed for various hydrocolloids (Fig. 5). The length of the boundary regime for samples with PS (sample 8), CS (sample 9), and high WPI levels (sample 10) was similar to that of the control sample (sample 1). This result was likely due to the larger size of the WPI, SMP, and starch molecules. These molecules would not be able to fit between the PDMS surface and balls when the gap between these contacting surfaces was small at low siding speeds, resulting in similar friction behavior to that of the control sample at

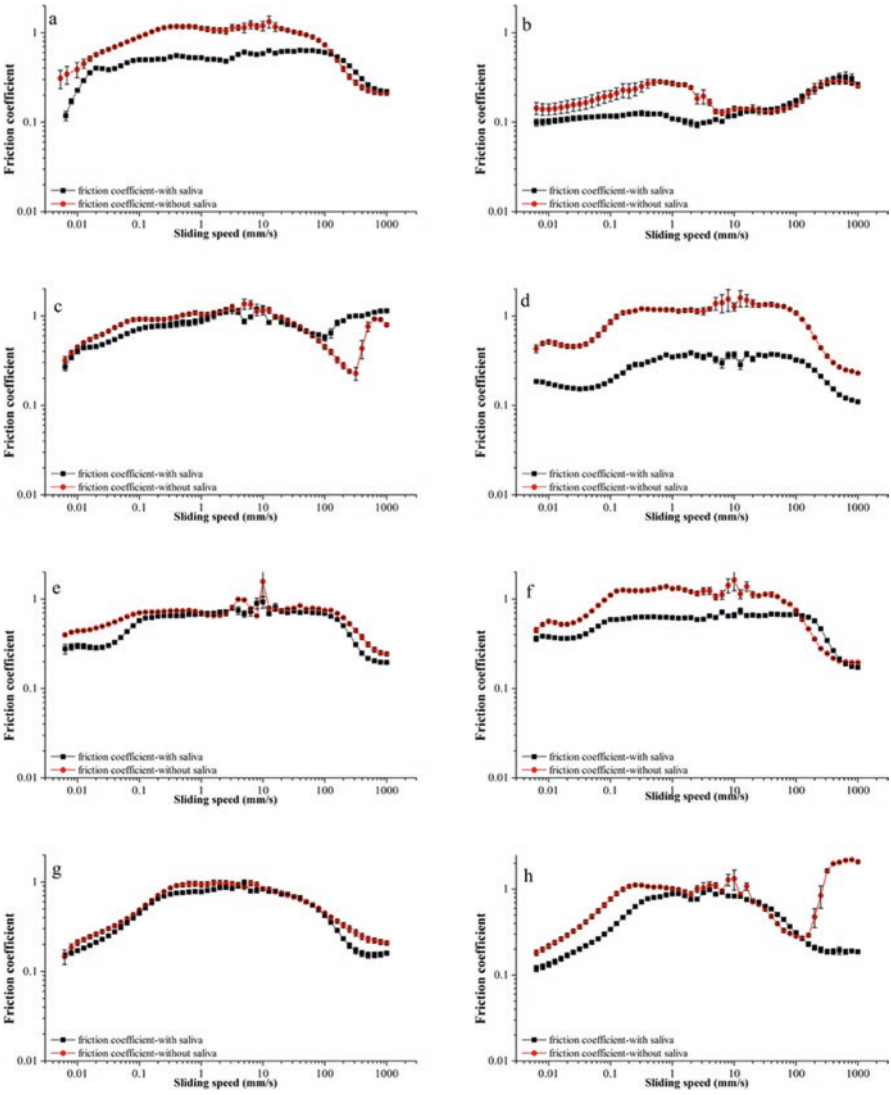

Fig. 5 Tribological results of yogurts; (**a**) sample 1 (control); (**b**) sample 4; (**c**) sample 6; (**d**) sample 7; (**e**) sample 8; (**f**) sample 9; (**g**) sample 10; (**h**) sample 12

those speeds. Sample 4 (full fat sample) showed a friction curve shape that was distinctly different from those of the other samples, likely due to its milkfat content. Part of hydrodynamic region can be seen at the end of the mixed regime for this sample when HWS was not added to the sample. Samples containing CMC (sample 7) and all hydrocolloids (sample 12) had similar friction curves, as did the control sample (sample 1) and samples containing PS (sample 8), CS (sample 9), and high levels of WPI (sample 10). Samples 7 and 12 also had similar phase angles (Table 7)

and microstructures (Figs. 2 and 3). The friction curves for samples 6 and 7 were notably different in their shape. Addition of LBG (sample 6) caused higher friction coefficients than addition of CMC (sample 7). This result was likely due to the type of microstructures that LBG and CMC formed in the yogurt systems. The small, aggregated LBG molecules dispersed throughout the protein network would have been easier to deform and made a more particulate microstructure compared to the cohesive microstructure formed with addition of CMC. Samples with added LBG (sample 6), CMC (sample 7), and all hydrocolloids (sample 12) transitioned to the mixed regime at lower sliding speeds compared to the control sample (sample 1) and the samples with added PS (sample 8) or CS (sample 9). Among all samples, the full-fat sample (sample 4) showed a transition to the mixed regime at the lowest sliding speed. Samples with added LBG (sample 6), CS (sample 9), and all hydrocolloids (sample 12) had the least changes in their friction profiles after addition of HWS, which was in agreement with microscopy and rheological results. LBG, used in sample 6, is a neutral polysaccharide that has been shown to be less affected by HWS than other hydrocolloids (Zinoviadou et al. 2008). The effect of HWS on the friction behavior of CMC was greater than that for LBG. Addition of HWS to samples containing PS (sample 8) resulted in a drastic decrease in friction coefficients compared to samples made with CS (sample 9). This effect was attributed to the lower amylose content and larger granule size and branched microstructure of PS compared to CS, as discussed in the previous section (Sect. 3.3.2). However, these samples showed similar friction profile shapes.

Overall, the friction behaviors of yogurts changed with formulation and addition of HWS. Correlation of these observations with sensory results can be helpful to decide whether using HWS is necessary in tribometry to determine relationships between friction behaviors and sensory texture. These correlations will be discussed in Sect. 3.7.

3.5 Effect of Formulation and HWS on Yogurt Texture Attributes

Formulation, panelist, and their interaction showed significant influence on most yogurt textural attributes at $p \leq 0.001$. Panelist affected sliminess at $p \leq 0.01$, the interaction of panelist and formulation affected chalkiness afterfeel at $p \leq 0.05$, and none of these factors had a significant effect on spoon viscosity (Table 12). These results indicated that all factors evaluated contributed significantly to the variance in sensory scores. There were no significant differences between replicates or for any interaction term containing replicates, indicating that replicates did not contribute significantly to the variations in scores.

Significant differences among samples for texture attributes were found for every texture attribute measured (Table 13), which was not surprising given the variation in the samples' microstructural, rheological, and tribological results. Samples with-

out gums and starches (samples 1–5) showed the highest spoon lumpiness. These samples contained SMP (sample 1), low levels of WPI (sample 5) and different fat ratios (samples 2, 3, and 4). Spoon lumpiness intensity significantly decreased when WPI was used in a higher ratio and without addition of SMP (sample 10), as well as when LBG (sample 6), CS (sample 9), or a combination of all hydrocolloids (sample 12) were used. Addition of milk-based additives can cause unpleasant texture attributes in yogurts (Morell et al. 2015). This has been attributed to protein aggregation and a possibility of two different protein matrices, one formed by the native milk proteins and the second by the added proteins (Morell et al. 2015). Using polysaccharide-based hydrocolloids, on the other hand, can provide a smoother texture. Unsurprisingly, lumpiness in mouth followed similar trends as spoon lumpiness.

Samples with added LBG (sample 6), CMC (sample 7), and all hydrocolloids (sample 12) had the highest degree of mouthcoat. Mouthcoating was significantly lower in the sample with high levels of WPI (sample 10), the low-fat sample (sample 2) and the sample with added PS (sample 8). Samples 1, 3, 4, and 5 were not significantly different from samples 2 and 8 for intensity of mouthcoat. The lack of mouthcoating in samples containing starches was likely due to the role of amylase in starch breakdown. This effect was noted by De Wijk et al. (2009). The low mouthcoating for the sample containing high levels of WPI may be due to its high melting attribute, which would remove the feeling of a coating on the oral surfaces due to rapid meltaway. Attribute scores for samples 1–5 (control sample, samples containing fat, and sample with low levels of WPI) showed that the effects of SMP were

Table 12 Main sources of variation of textural attributes of yogurt ($n = 12$) determined by F-values obtained from three-way ANOVA[a]

Sources	Formulation	Replicate	Panelist	Formulation × Replicate	Panelist × Replicate	Panelist × Formulation
Spoon viscosity	73.39***	13.01	17.96***	1.23	1.3	1.23
Graininess	85.45***	3	40***	0.69	1.02	4.34***
Mouthcoat	33.06***	2.36	18.73***	0.65	1.03	2.83***
Firmness	74.73***	2.37	29.12***	2.84	2.23	4.66***
Mouth viscosity	98.19***	0.13	22.13***	0.59	1.08	5.2***
Lumpiness	161.4***	3.48	40.37***	1.8	0.69	4.8***
Lumpiness in mouth	178.91***	0.04	56.11***	2.72	1.24	5.45***
Smoothness	119.99***	0.06	42.71***	1.74	0.68	4.61***
Melting	29.94***	1.98	38.3***	1.74	1.05	4.45***
Grittiness	21.74***	0.41	22.76***	2.08	0.8	2.51***
Astringency	16.36***	1.41	58.82***	1.15	0.98	2.48***
Chalkiness afterfeel	13.13***	0.08	13.82***	0.72	0.85	1.79*
Sliminess	83.7***	2.3	6.97**	1.9	1.07	4.72***

[a]*, **, and *** indicate significant differences at $p \leq 0.05$, $p \leq 0.01$, and $p \leq 0.001$, respectively

Table 13 Yogurt sensory attributes as evaluated by trained panelists[1]

Formula number	Attribute number[2]												
	1	2	3	4	5	6	7	8	9	10	11	12	13
1	10.0^{a}	4.05^{d}	7.28^{b}	3.79^{c}	3.16^{cd}	3.81^{bc}	8.53^{a}	3.49^{d}	7.00^{bc}	5.09^{a}	5.94^{a}	4.16^{ab}	1.78^{c}
2	10.6^{a}	3.82^{d}	6.96^{b}	3.53^{cd}	2.94^{cd}	3.48^{bc}	8.49^{a}	3.45^{d}	7.12^{bc}	4.69^{ab}	5.85^{a}	3.98^{ab}	1.88^{c}
3	10.5^{a}	3.68^{d}	6.18^{b}	3.84^{c}	3.02^{cd}	3.47^{bc}	8.38^{a}	3.77^{d}	7.58^{b}	4.46^{ab}	5.76^{a}	4.13^{ab}	1.91^{c}
4	9.82^{a}	4.07^{d}	5.91^{bc}	3.98^{c}	3.33^{cd}	3.45^{bc}	7.85^{a}	4.00^{d}	7.61^{ab}	4.52^{ab}	5.32^{ab}	4.40^{ab}	1.97^{c}
5	10.4^{a}	3.86^{d}	6.48^{b}	3.75^{c}	3.06^{cd}	3.49^{bc}	8.15^{a}	3.71^{d}	7.51^{bc}	4.7^{ab}	5.80^{a}	4.21^{ab}	1.98^{c}
6	4.67^{c}	7.30^{b}	9.64^{a}	6.28^{a}	6.67^{a}	5.76^{a}	4.54^{b}	3.31^{d}	4.40^{e}	4.31^{ab}	4.32^{bcd}	3.68^{bc}	3.39^{b}
7	2.53^{d}	7.63^{ab}	2.51^{d}	5.38^{ab}	6.70^{a}	5.52^{a}	1.93^{d}	10.1^{a}	5.23^{cde}	2.19^{c}	3.77^{cd}	2.38^{c}	4.58^{a}
8	6.97^{b}	3.37^{de}	3.79^{d}	3.29^{cd}	2.92^{cd}	2.8^{dc}	4.07^{bc}	6.94^{c}	9.00^{ab}	3.57^{bc}	5.69^{a}	3.60^{bc}	1.82^{c}
9	$5.5b^{c}$	5.69^{c}	$4.15d^{c}$	4.45^{bc}	4.92^{b}	4.16^{b}	2.95^{bcd}	7.66^{bc}	6.80^{bcd}	4.76^{ab}	5.60^{ab}	4.51^{ab}	2.38^{c}
10	4.58^{c}	2.44^{e}	2.66^{d}	2.39^{d}	2.13^{d}	2.03^{d}	2.21^{d}	8.99^{ab}	9.93^{a}	2.75^{c}	5.56^{ab}	2.40^{c}	1.65^{c}
11	2.53^{d}	3.86^{d}	9.40^{a}	4.03^{c}	3.61^{bc}	2.94^{dc}	2.73^{cd}	3.31^{d}	8.21^{ab}	5.60^{a}	4.96^{abc}	5.36^{a}	3.30^{b}
12	3.77^{cd}	8.46^{a}	3.95^{d}	5.84^{a}	6.91^{a}	6.15^{a}	2.36^{cd}	9.07^{ab}	4.56^{de}	2.51^{c}	3.49^{d}	2.56^{c}	4.44^{a}

[1]Letters in each column that are significantly different indicate significant differences

[2]Attributes include: (1) Spoon lumpiness; (2) Spoon viscosity; (3) Graininess; (4) Mouthcoat; (5) Mouth viscosity; (6) Firmness; (7) Lumpiness in mouth; (8) Smoothness; (9) Melting; (10) Grittiness; (11) Astringency; (12) Chalkiness afterfeel; (13) Sliminess

dominant to those of the milkfat content in perceived sensory texture. SMP is a popular additive that is used to alter yogurt texture (Karam et al. 2013) through short chains of proteins in the system. The bonds between these chains can easily break once the product is in the mouth, resulting in a low mouthcoat; longer protein chains are needed to provide a more substantial mouthcoat.

Increased astringency, grittiness, and graininess due to addition of SMP and WPI in the yogurt samples may have been due to increased particle size when these proteins were added to the yogurt system, resulting in a higher sensation of astringency, grittiness, and graininess (Sano et al. 2005; Andrewes et al. 2011). Another reason for the increased astringency, grittiness, and graininess could be aggregation of milk proteins with themselves or with saliva. Sliminess and ropiness are attributes that can be caused by exopolysaccharide- (EPS-) producing bacteria. The EPS can have negative or neutral charges based on the strains of bacteria (van de Velde et al. 2015). Thus, EPS can form long chains with milk proteins, resulting in a long, stringy texture. The mechanism of EPS interaction with milk proteins has been shown to be similar to the interaction mechanism of milk proteins with added hydrocolloids. Samples containing CMC (sample 7) and all hydrocolloids (sample 12) showed the highest intensity of sliminess, probably due to the presence of CMC, which has an opposite charge to that of milk proteins. These electrostatic interactions, as well as hydrophobic interactions, can form longer chains of proteins and cause a slimier texture. It appeared that the presence of strong interactions was required for this attribute in the yogurt samples since samples with LBG (sample 6), a neutral hydrocolloid with weak bonds to protein, had significantly lower sliminess than sample 7 or 12.

Overall, samples 7 (CMC) and 12 (all hydrocolloids) showed similar attribute trends. For instance, spoon viscosity, firmness, and viscosity in mouth had the greatest intensity and graininess, chalkiness, and grittiness had the lowest intensity for both samples. These results suggest that yogurts formulated with either CMC or a combination of all hydrocolloids used in this study had the most positive combination of texture attributes. The suitability of these combinations have also been shown in other studies (Alakali et al. 2008; Murray and Phisarnchananan 2014).

3.6 Principal Component Analysis of Sensory Results

Principal component analysis (PCA) was performed to visualize the relationships between the samples and their textural attributes (Fig. 6). The first two principal components accounted for 59.9% and 26.3% of the variance, respectively, in the 13-variable system. The attributes most negatively correlated with PC1 were mouth viscosity, spoon viscosity, sliminess, and firmness. The most positive correlations to PC1 were for astringency and low-melting. PC2 was positively correlated with graininess and negatively correlated with smoothness. The results from this plot were in accordance with the results for the sensory attributes (Table 13).

A cluster analysis of the 13 textural attributes of all yogurts showed the yogurts fit into one of three groups, designated by the colors of the circles in the PCA plot (Fig. 6). The first cluster (green) had two main subgroups: (1) samples 7, 9, and 12, and (2) samples 8 and 10. Samples 7, 9, and 12 were positively described by smoothness, sliminess, both viscosity-related attributes, firmness, and mouthcoating but negatively related to astringency and low-melting. Samples 8 and 10 showed the opposite relationships. As explained in Sect. 3.5, the CMC in sample 7 and all hydrocolloids in sample 12 had the greatest contribution to these attributes due to a higher number of electrostatic and hydrophobic interactions, as well as covalent bonds formed by CMC and PS, which are negatively charged hydrocolloids (Alakali et al. 2008). Additionally, samples 7 and 12 showed the highest intensities of ideal texture attributes (see Sect. 3.5), which was attributed to the addition of CMC. The palatability of the yogurt produced with CS (sample 9) was likely caused by its structural features (Alakali et al. 2008). CS granules are small compared to PS granules, and they can reduce the sensation of dryness in the mouth. Alakali et al. (2008) suggested that the residual corn oil in CS may also be partially responsible for the palatability of CS-containing yogurts.

The second cluster (red) included samples 6 (containing LBG) and 11 (containing LBG and CS). Sample 6 was positively related to most of the attributes that were positively related to the first cluster (green) and negatively related to lumpiness-related attributes, graininess, low-melting, and astringency. In the LBG-containing samples, the neutral LBG would increase the viscosity of the continuous phase,

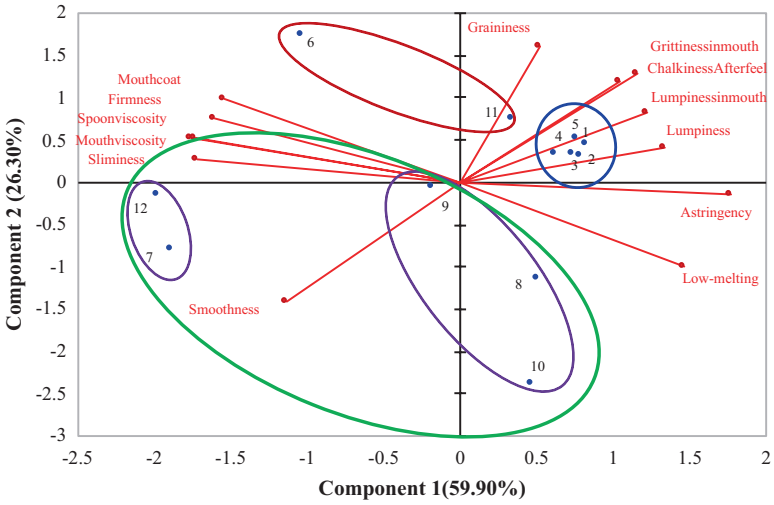

Fig. 6 Principal Component Analysis (PCA) biplot for texture attributes of yogurts (n = 12) analyzed by descriptive sensory panelists (n = 10). Clusters have been circled based on cluster analysis

promoting these attributes (Thaiudom and Goff 2003). Sample 11 was positively related to lumpiness-related attributes, graininess, low-melting, and astringency. However, the intensity of these undesirable defects was significantly lower than those of samples 8 and 10 in the green cluster. The presence of CMC was hypothesized to be the reason for this result.

The third cluster (blue) consisted of samples 1, 2, 3, 4, and 5 (control, fat-containing samples, and low-level WPI-containing sample, respectively). These samples were mostly related to grittiness, chalkiness afterfeel, both lumpiness attributes, graininess, and astringency. SMP was the common additive in these samples. Addition of milk powders, e.g. SMP and WPI, is known to increase the intensity of these attributes (Isleten and Karagul-Yuceer 2006). Overall, the combination of PCA and cluster analysis helped illustrate significant attributes as well as trends among samples.

3.7 Correlations Among Yogurt Rheological, Tribological, and Texture Behaviors

3.7.1 Correlations Among Yogurt Textural Attributes

Multiple significant correlations were found among textural attributes (Table 14). There were two major groups of attributes in this matrix. The first group included negative texture attributes: spoon and mouth lumpiness, low-melting, grittiness, astringency, and chalkiness afterfeel. As expected, these negative attributes showed negative correlations with the second group of more palatable attributes: spoon viscosity, mouthcoat, mouth viscosity, firmness, smoothness, and sliminess. The overall drivers behind these attributes included particle size, structural features, and changes to structural features, upon contact with HWS.

As expected, the highest correlations were between spoon lumpiness and mouth lumpiness, as well as spoon viscosity and mouth viscosity. This result was likely due to the fact that appearance may highly affect other senses; i.e., the appearance of the sample impacted its in-mouth perception, or the intensity of these attributes in the mouth remained similar to those of their appearance. Viscosity-related attributes had the highest number of correlations to other attributes. In terms of the undesirable attributes, astringency and lumpiness had the highest correlation. These results emphasize that yogurt textural attributes can be related to each other, potentially due to structural features that have a variety of effects. Therefore, care must be taken in formation of new yogurt products so that formulation changes to address issues with one textural attribute does not cause undesirable changes in a second attribute.

Table 14 Correlation matrix for yogurt textural attributes[a]

Attribute	Spoon lumpiness	Spoon viscosity	Graininess	Mouthcoating	Mouth viscosity	Firmness	Lumpiness in mouth	Smoothness	Melting	Grittiness	Sliminess
Spoon viscosity	−0.534*	1.00			0.991***				−0.942***		
Mouthcoat		0.953***		1.00					−0.961***		
Mouth viscosity	−0.609*	0.991***		0.958***	1.00				−0.920***		
Firmness		0.975***		0.958***	0.953***	1			−0.986***		
Lumpiness in mouth	0.955***										
Smoothness	−0.602*		−0.893***				−0.761**			−0.878**	
Low-melting		−0.942***		−0.961***	−0.920***	−0.986***					
Grittiness			0.814**				0.548*	−0.878**	1.00	1.00	
Astringency	0.740**	−0.884***		−0.822**	−0.896**	−0.809**	0.628*		0.750**	0.562*	−0.964***
Chalkiness afterfeel			0.727**					−0.785**		0.960***	
Sliminess	−0.745**	0.884***		0.829**	0.900***	0.808**	−0.614*		0.761**		1.00

[a]Only significant correlations at $^{*}p \leq 0.01$ $^{**}p \leq 0.001$; $^{**}p \leq 0.0001$ are shown

Table 15 Correlation among yogurt flow and viscoelastic parameters[a]

Formula	η_o at 8 °C no HWS	η_o at 25 °C no HWS	c at 25 °C no HWS	n at 8 °C no HWS	η_o at 8 °C HWS	η_o at 25 °C HWS	c at 8 °C HWS	n at 25 °C HWS
G^*, 8 °C, no HWS	***0.985	***0.980	*0.817					
G^*, 25 °C, no HWS	*0.892	**0.900	*0.855					
tan δ, 8 °C, no HWS				*-0.676				
tan δ, 25 °C, no HWS				*-0.650				
G^*, 8 °C, HWS					*0.864	*0.780		
G^*, 25 °C, HWS					*0.844	*0.791		
γ_c, 25 °C, HWS							*0.712	*0.628

[a]Only significant correlations at $^*p \leq 0.05$; $^{**}p \leq 0.01$; $^{***}p \leq 0.001$, are shown

3.7.2 Correlations Among Yogurt Viscoelastic and Flow Behaviors

Correlations were found among yogurt viscosity and viscoelastic behaviors for samples with and without added HWS (Table 15). G^* was significantly correlated with η_o and c at 8 and 25 °C, and tan δ was only correlated to G^* and η_o at 8 °C without HWS application. These results showed with increasing G^*, η_o also increased. These correlations were reflected in the viscosity and strain sweep results: samples with higher tan δ had lower η_o values. Thus, the greater the values of η_o, the more solid-like behavior the material exhibited. When samples were tested with addition of saliva, G^* was correlated to η_o at both 8 and 25 °C, but tan δ showed no significant correlation with any other parameter. Critical strain correlated to n and c from viscosity parameters: samples with increased critical strain also had higher n and c values. Overall, addition of HWS did have some impact on the correlations found among rheological parameters, suggesting that incorporation of HWS may impact relationships among sample rheological behaviors. This was not surprising considering the impact of HWS on yogurt microstructures (Sect. 3.2).

Tribological results were negatively correlated to yogurt viscosity parameters, including n when HWS was not added and both c and n with added HWS (Table 16). The correlations were found at all selected sliding speeds (10–100 mm s^{-1}) for n with added HWS and all selected sliding speeds but 1 mm s^{-1} for c with added HWS and n when HWS was not added.

In general, increased shear-thinning behavior, potentially due to weaker microstructures, resulted in higher friction coefficients. The correlations of c with tribological results when HWS was added suggested that addition of HWS to samples for testing can strengthen the correlations between flow properties and friction

Table 16 Correlations among yogurt friction coefficients and flow parameters[a]

Friction coefficients (μ) with HWS												
Viscosity parameters	μ at 1 mm s^{-1}	μ at 5 mm s^{-1}	μ at 10 mm s^{-1}	μ at 15 mm s^{-1}	μ at 20 mm s^{-1}	μ at 25 mm s^{-1}	μ at 30 mm s^{-1}	μ at 40 mm s^{-1}	μ at 50 mm s^{-1}	μ at 60 mm s^{-1}	μ at 80 mm s^{-1}	μ at 100 mm s^{-1}
n with HWS	−0.702*	−0.701*	−0.675*	−0.66*	−0.655*	−0.652*	−0.65*	−0.648*	−0.647*	−0.647*	−0.646*	−0.645*
c (s) with HWS		−0.609*	−0.592*	−0.583*	−0.581*	−0.58*	−0.58*	−0.578*	−0.577*	−0.577*	−0.577*	−0.577*
n no HWS		−0.797**	−0.852***	−0.878***	−0.888***	−0.891***	−0.893***	−0.894***	−0.9***	−0.9***	−0.9***	−0.9***

[a]Only significant correlations at $^{*}p \leq 0.05$; $^{**}p \leq 0.01$; and $^{***}p \leq 0.001$ are shown

coefficients. However, there were no correlations between η_o and friction coefficients at any sliding speed. In addition, no significant correlations were found among yogurt viscoelastic and friction behaviors. This result was not expected as some viscoelastic properties, e.g. viscoelastic moduli or tan δ, have been found to be related to friction behavior in other studies (Chen and Engelen 2012). The lack of correlation in this study implied that structural features that control viscoelastic properties in these samples may not have significant impact on friction behaviors and vice versa.

3.7.3 Correlations Among Yogurt Flow Parameters and Textural Behaviors

Viscosity parameters and sensory results showed few correlations. However, η_o was positively correlated with firmness at 25 °C ($R^2 = 0.87$) and n was negatively correlated with sliminess at 8 °C ($R^2 = 0.88$) when HWS was added. Firmer yogurts showed higher instrumental viscosity, since a greater force was needed to induce flow. Firmer materials would have stronger bonds and other intermolecular interactions, making their microstructures more resistant to flow. As previously discussed, sliminess is the result of strong interactions between milk proteins and hydrocolloids. Slimy materials typically show shear-thinning behavior; this behavior can be intensified by addition of long-chain, proline-rich mucins and other salivary proteins. c was negatively correlated with low-melting ($R^2 = 0.930$), grittiness ($R^2 = 0.822$), and astringency ($R^2 = 0.844$) at 8 °C when HWS was not added. The parameter c is the time needed for a material to flow and is known to be increased by protein aggregations or larger particle sizes (Genovese et al. 2007). Therefore, more time is needed to disrupt stronger microstructures or larger molecules through shear.

3.7.4 Correlations Among Yogurt Viscoelastic and Textural Behaviors

Viscoelastic parameters that correlated with yogurt texture attributes included only tan δ at γ_c obtained from strain sweep data. Neither γ_c nor G^* at γ_c showed significant correlations with sensory terms (Table 17). tan δ was positively correlated with viscosity-related attributes, mouthcoat, firmness, and sliminess. It was also negatively correlated with low-melting, lumpiness, and astringency. As tan δ increases, materials show more viscous-type behavior; i.e., they flow more readily under their own weight. A potential explanation for the correlation of tan δ with firmness and viscosity is that panelists may have interpreted the increased fluid-like behavior as increased viscosity, sliminess, and mouthcoat. Correlations at different temperatures were not significantly different. This was attributed to the short time semisolid foods are held in the mouth before swallowing.

Table 17 Correlations among yogurt viscoelastic parameters and sensory attributes[a]

Viscosity parameters	Spoon lumpiness	Spoon viscosity	Mouth-coat	Mouth viscosity	Firm-ness	Low-melting	Astrin-gency	Slimi-ness
tan δ (rad) at 8 °C, no HWS	−0.695*	0.702*	0.783*	0.750*	0.656*	−0.663*	−0.832**	0.860**
tan δ (rad) at 8 °C, with HWS	−0.698*						−0.626*	0.706*
tan δ (rad) at 25 °C, no HWS	−0.690*	0.748*	0.807*	0.787*	0.710*	−0.710*	−0.870**	0.886**
tan δ (rad) at 25 °C, with HWS	−0.708*						−0.654*	0.734*

[a]Only significant correlations at $^{*}p \leq 0.05$; $^{**}p \leq 0.01$; and $^{***}p \leq 0.001$ are shown

3.7.5 Correlations Among Yogurt Frictional and Textural Behaviors

Friction coefficients of yogurts at 1–100 mm s^{-1} sliding speeds were correlated with sensory results at 25 °C (Table 18). These sliding speeds were selected since oral sliding speeds have been reported to be in the range of 10–100 mm s^{-1} (Malone et al. 2003). The lower sliding speeds were selected to account for some of the slower movements used while evaluating food texture.

Spoon lumpiness was positively correlated to friction coefficient at all sliding speeds, excluding 1 and 5 mm s^{-1} for friction coefficients measured without HWS, and excluding 1 mm s^{-1} for friction coefficients measured with added HWS. Friction coefficients with and without saliva at 1 mm s^{-1} were correlated with mouth viscosity and smoothness. Negative correlation of smoothness with friction coefficient were expected: smoother yogurts would have lower friction coefficients due to the lack of large particles or lumps. Mouth viscosity was positively correlated with friction coefficients at 60, 80, and 100 mm s^{-1} when no HWS was added during tribological testing. This result was opposed to the findings for model hydrocolloid solutions (De Vicente et al. 2006). However, the positive correlation between viscosity and friction has been found in a more recent study on semisolid dairy products (Sonne et al. 2014). The conflicting results may be due to the larger particle sizes in semisolid foods with higher protein content compared to that of oil-in-water emulsions, particularly if WPI is used as the protein source (Krzeminski et al. 2011). The protein molecules might be trapped between or adhere to the two sliding surfaces, increasing the friction during sliding.

Table 18 Correlations among sensory attributes and friction coefficients of yogurts with and without HWS addition at 25 °C ($n = 12$)[a]

Sensory attributes	μ at 1 mm s^{-1}	μ at 5 mm s^{-1}	μ at 10 mm s^{-1}	μ at 15 mm s^{-1}	μ at 20 mm s^{-1}	μ at 25 mm s^{-1}	μ at 30 mm s^{-1}	μ at 40 mm s^{-1}	μ at 50 mm s^{-1}	μ at 60 mm s^{-1}	μ at 80 mm s^{-1}	μ at 100 mm s^{-1}
Correlations with HWS												
Lumpiness		0.615*	0.990***	0.997***	0.999***	0.999***	0.999***	0.999***	0.999***	0.999***	0.999***	1.00***
Spoon viscosity	−0.840**	−0.692*										
Smoothness	−0.902***	−0.684*										
Low-melting	0.617*											
Mouth viscosity												
Correlations without HWS												
Lumpiness			0.914***	0.967***	0.992***	0.996***	0.998***	0.998***	0.999***	0.999***	0.999***	0.999***
Spoon viscosity	−0.840**											
Smoothness	−0.902***											
Low-melting	0.616*											
Mouth viscosity										0.577*	0.579*	0.581*

[a]Only significant correlations at $^{*}p \leq 0.05$; $^{**}p \leq 0.01$; and $^{***}p \leq 0.001$ are shown

4 Comparison of Yogurt and Acid Milk Gel Microstructures, Rheological and Tribological Behaviors, and Texture Attributes

Acid milk gels are often used as an analog for yogurts since controlling the final pH and time to reach final pH is easier with a chemical acidifier, e.g. GDL, compared to using live bacteria. However, using different methods of chemical and biological acidification may result in notable differences in gel microstructure and physicochemical, functional, and textural behaviors of the products. Therefore, this section compares the microstructural features and rheological, tribological, and sensory behaviors of acid milk gels (full data set presented in Chapter 11) and yogurts to determine the differences between these two systems and assess the suitability of acid milk gels as an analog for yogurts. Table 19 presents the acid milk gel formulations used for comparison with the yogurts.

Table 19 Acid milk gel formulations used for comparison to yogurts

Formula number used in this chapter	Formula number used in Chap. 11	SMP (w/w)	WPI (w/w)	LBG (w/w)	CMC (w/w)	Potato starch (w/w)	Corn starch (w/w)	Skim milk (w/w)	Cream (w/w)	GDL (w/w)
1	1	2.8	0	0	0	0	0	97.2	0	1.1–1.55
2	2	2.83	0	0	0	0	0	95.96	1.21	1.1–1.55
3	3	2.89	0	0	0	0	0	92.26	4.85	1.1–1.55
4	4	2.95	0	0	0	0	0	89.15	7.9	1.1–1.55
5	5	1.8	1	0	0	0	0	97.2	0	1.1–1.55
6	6	1.8	0	1	0	0	0	97.2	0	1.1–1.55
7	7	1.8	0	0	1	0	0	97.2	0	1.1–1.55
8	8	2.1	0	0	0	0.7	0	97.2	0	1.1–1.55
9	9	2.1	0	0	0	0	0.7	97.2	0	1.1–1.55
10	16	0	2.8	0	0	0	0	97.2	0	1.1–1.55
11	18	0	0	1.8	0	0	1	97.2	0	1.1–1.55
12	24	0.2	0.8	0.45	0.45	0.45	0.45	97.2	0	1.1–1.55

4.1 Microstructural Comparison

Comparing the microstructural images of acid milk gels to their yogurt counterparts showed only slight differences. The protein network of yogurts showed slightly more open and larger strands, chains, and clusters for most of the formulations compared to their acid milk gel analogues. This result was attributed to rate of acidification from lactic acid bacteria (LAB) versus GDL to form the protein matrices in these systems. During acidification, GDL is hydrolyzed to gluconic acid to lower the pH in acid milk gels. On the other hand, LAB consume lactose as a source of sugar to produce lactic acid. Both acids lower the pH, resulting in aggregation and gelation of milk proteins. However, LAB typically produce lactic acid at a slower rate than GDL dissociation, resulting in a longer gelation time for yogurt compared to that for acid milk gels (Lucey et al. 1998). Gelation time was considered to be the time needed to reach a pH between 4.55 and 4.6 (casein's isoelectric point). Acid milk gels had a 4 h gelation time; yogurts had a 4–6 h gelation time. Gelation time was optimized based on the control sample formation for acid milk gels. However, gelation time differed among the various formulations of yogurts due to variations in LAB activity and different amount of starter culture added to account for formulation differences per the manufacturer's instructions.

At pH between 4.55 and 4.6 for both acid milk gels and yogurts, electrostatic and protein–protein attractions occurred through hydrophobic interactions to form the protein matrix throughout the gel (Lee and Lucey 2004). In this protein network, casein micelles are linked by protein clusters and chains that are distributed in a serum phase with void pores or pores in which the aqueous phase is trapped (Lee and Lucey 2010). This matrix was shown to be similar in acid milk gels and yogurts.

4.2 Rheological and Tribological Behavior Comparison

Overall, there were no significant differences ($p > 0.05$) among the zero shear viscosity values of the yogurts and acid milk gels at 8 and 25 °C based on the results of a two-tailed *t*-test. Both acid milk gels and yogurts showed shear-thinning behavior, but their viscosity curves were best fit to different flow behavior models. The differences in the flow behavior results can be explained by microstructural differences and longer yogurt gelation time. Slow acidification can provide better conditions for protein interaction, strengthening the gel network and increasing viscosity (Martin et al. 1999; Lee and Lucey 2006), as well as promoting structural features that are slower to break down under shear. Accordingly, most yogurt formulations had moderately larger protein clusters and more even protein–protein crosslinking compared to their acid milk gel analogues. Additionally, the comparison of *n* values of yogurts and their acid milk gel analogues obtained from the flow behavior models showed no significant differences at 8 and 25 °C ($p > 0.05$). This result was reflected in the similar shapes of the yogurt and acid milk gel viscosity profiles (examples shown in

Fig. 7). Yogurt and acid milk gel strain sweep data also showed similar patterns (examples shown in Fig. 8). Additionally, yogurt viscoelastic properties, including γ_c, G'', and G^*, were not significantly different from their acid milk gel analogues at both 8 and 25 °C ($p > 0.05$). Similarly, no significant differences were observed in acid milk gel and yogurt friction coefficients at selected sliding speeds at 25 °C ($p > 0.05$), and their friction profile shapes were similar (examples shown in Fig. 9).

4.3 Textural Attribute Comparison

Of all the textural attributes evaluated for the yogurts and acid milk gels, only graininess scores showed significant differences between similar yogurt and acid milk gel formulations ($p \leq 0.05$). Acid milk gels showed significantly lower graininess compared to yogurts. Interestingly, the longer yogurt gelation time did not appear to alter graininess intensity in yogurts versus acid milk gels. The most notable difference was shown for samples containing both LBG and CS (sample 11), which was

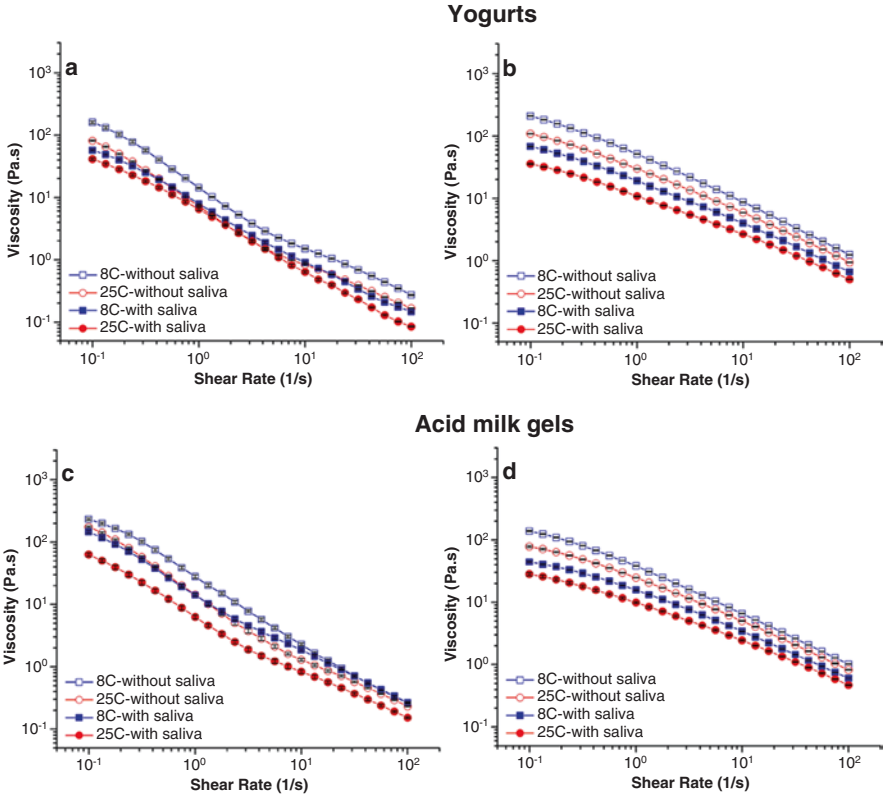

Fig. 7 Shear rate sweep results of two formulations of each of yogurts and acid milk gels. (**a**) sample 1; (**b**) sample 12; (**c**) sample 1; (**d**) sample 24. Formulations for acid milk gel samples are provided in Chap. 10

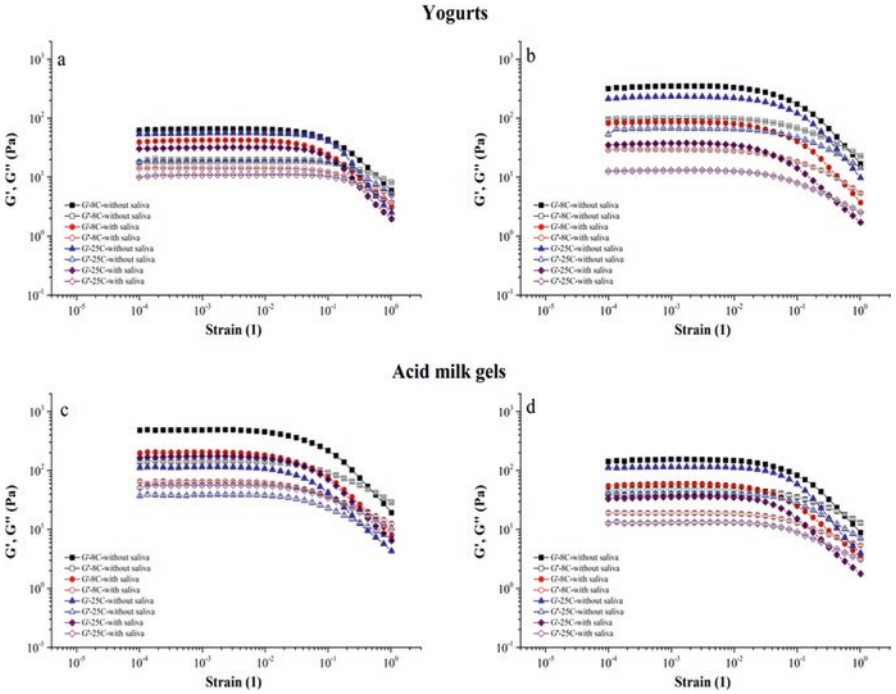

Fig. 8 Strain sweep results of two formulations of each of yogurts and acid milk gels. (**a**) sample 1; (**b**) sample 8; (**c**) sample 1; (**d**) sample 8. Formulations for acid milk gel samples are provided in Chap. 10

also reflected in the differences between the acid milk gel (Fig. 10) and yogurt (Fig. 6) PCA biplots.

Considering the sensory data for both acid milk gels and yogurts, samples 12 (all hydrocolloids added), 7 (added CMC), 6 (added LBG), and 11 (added LBG and CS) were the samples most related to the positive texture attributes, including mouth-coat, sliminess, spoon viscosity, firmness, mouth viscosity, and smoothness, for both acid milk gels and yogurts. The presence of at least one gum was hypothesized to be the main reason for improving the positive textural attributes. Samples formulated with CMC and all hydrocolloids had the lowest amount of astringency, likely because the hydrocolloids prevented HWS from interacting with whey proteins and causing an astringent sensation (Andrewes et al. 2011). Adding fat to samples 2, 3, and 4, and PS and CS to samples 8 and 9, respectively did not improve the textural attributes compared to the control (sample 1) in either yogurts and acid milk gels. Sample 8 (added PS) had high astringency and low-melting scores in both yogurts and acid milk gels. Sample 1 (control), and 5 (added WPI) were closest to lumpiness-related attributes along with chalkiness afterfeel, grittiness, and graininess. The least smooth samples were the control sample (sample 1), samples with added fat (samples 2, 3, and 4), and samples with added starch (samples 8 and 9) for both

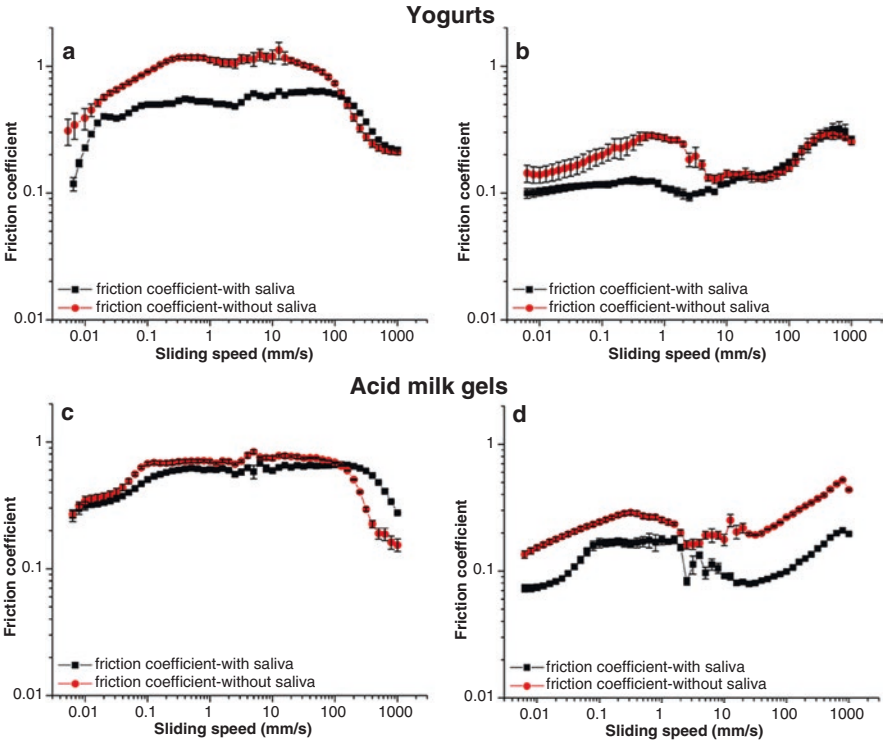

Fig. 9 Tribology results of two formulations of each of yogurts and acid milk gels. (**a**) sample 1; (**b**) sample 4; (**c**) sample 1; (**d**) sample 4. Formulations for acid milk gel samples are provided in Chap. 10

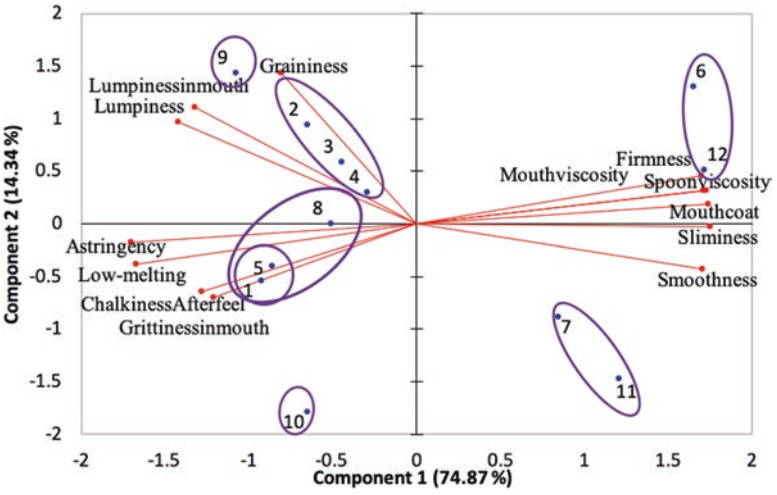

Fig. 10 Principal Component Analysis (PCA) biplot for texture attributes of acid milk gels (n = 12) analyzed by descriptive sensory panelists (n = 10). Clusters of samples determined from cluster analysis have been circled

yogurts and acid milk gels. Overall, the PCA plots showed that samples prepared with at least one gum (CMC or LBG) were associated with more desirable texture attributes, which was in line with the descriptive sensory results for both yogurts and acid milk gels.

5 Conclusions

Overall, the combination of rheology, tribology, sensory, and confocal imaging were found to be useful techniques for a deeper understanding of drivers of different yogurt textures. Addition of different hydrocolloids to the yogurt formulations significantly changed flow, viscoelastic, friction, and textural behaviors in yogurts. Microstructural images were a beneficial tool for determining protein network conformations, which showed relationships with multiple instrumental parameters and texture attributes. HWS had significant influence on all instrumental parameters and can be used to determine some of the mechanisms of food disruption when used during instrumental testing. However, correlations among yogurt rheological, tribological, and sensory behaviors did not significantly change for samples tested with or without HWS. More work is needed to understand the impact of HWS effects during oral processing and how HWS affects relationships between yogurt structures, mechanical behaviors, and sensory texture attributes.

The comparison of selected rheological parameters, tribological parameters, and sensory properties of acid milk gels and yogurts showed no significant differences, excluding the intensity of graininess in the textural attributes. Additionally, the patterns of their flow behavior, viscoelastic behavior, and friction profiles were also similar. However, small differences were observed for their sensory graininess and microstructures. This result was attributed to a longer gelation time for the LAB starter cultures compared to GDL. Therefore, acid milk gels can be considered an appropriate analog for yogurts that offers better control over final pH and gelation time.

Acknowledgements Funding for this project was provided by the USDA National Institute of Food and Agriculture (grant #2015-67018-23069).

Appendix

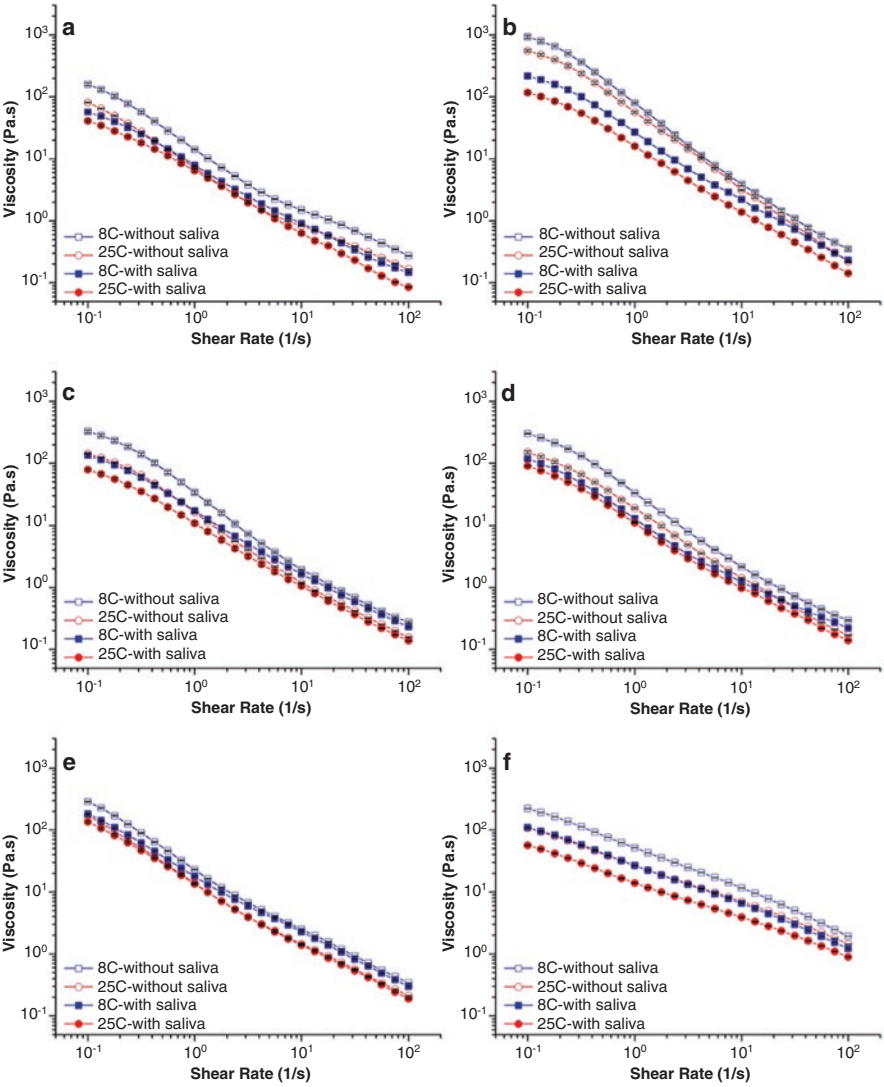

Fig. 11 Yogurt shear rate sweep results; (**a**) sample 1; (**b**) sample 2; (**c**) sample 3; (**d**) sample 4; (**e**) sample 5; (**f**) sample 6; (**g**) sample 7; (**h**) sample 8; (**i**) sample 9; (**j**) sample10; (**k**) sample 11; (**l**) sample 12

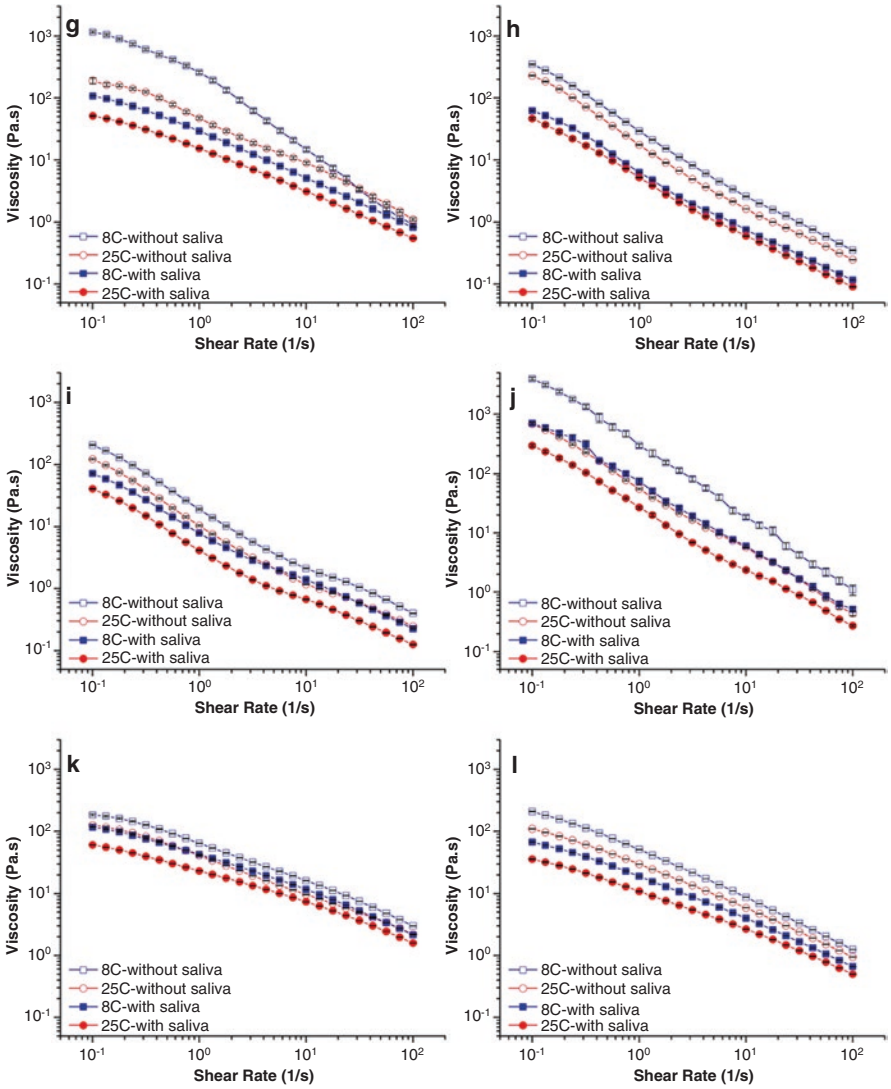

Fig. 11 (continued)

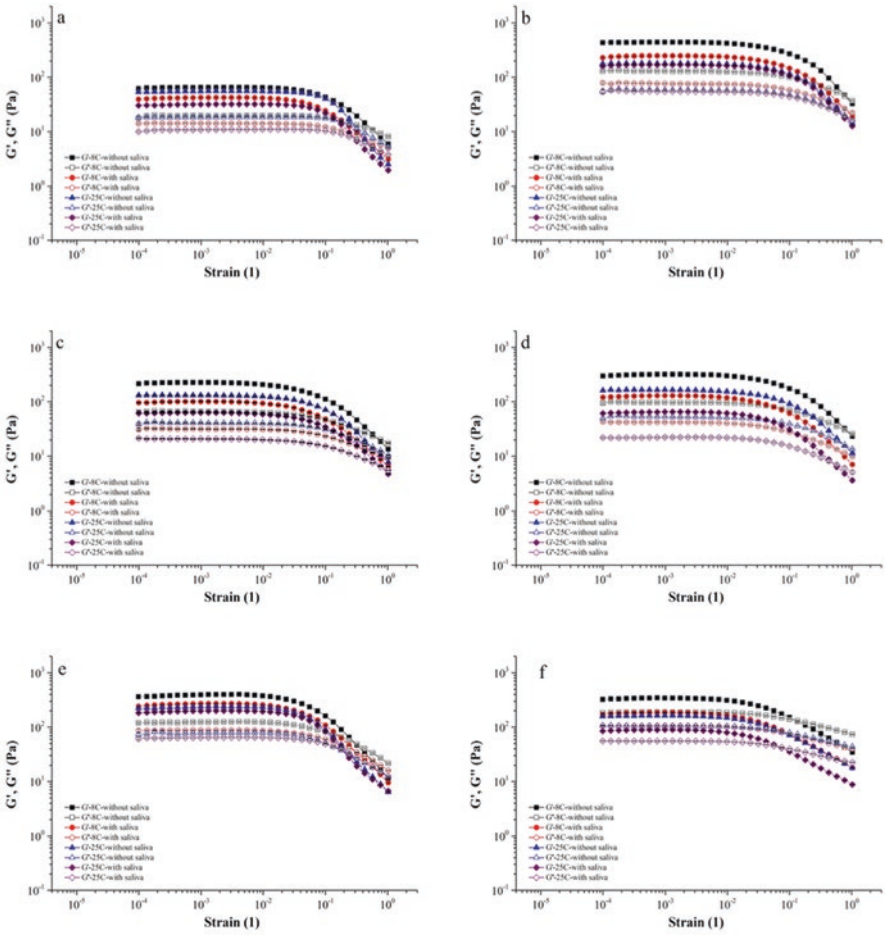

Fig. 12 Yogurt strain sweep results; (**a**) sample 1; (**b**) sample 2; (**c**) sample 3; (**d**) sample 4; (**e**) sample 5; (**f**) sample 6; (**g**) sample 7; (**h**) sample 8; (**i**) sample 9; (**j**) sample10; (**k**) sample 11; (**l**) sample 12

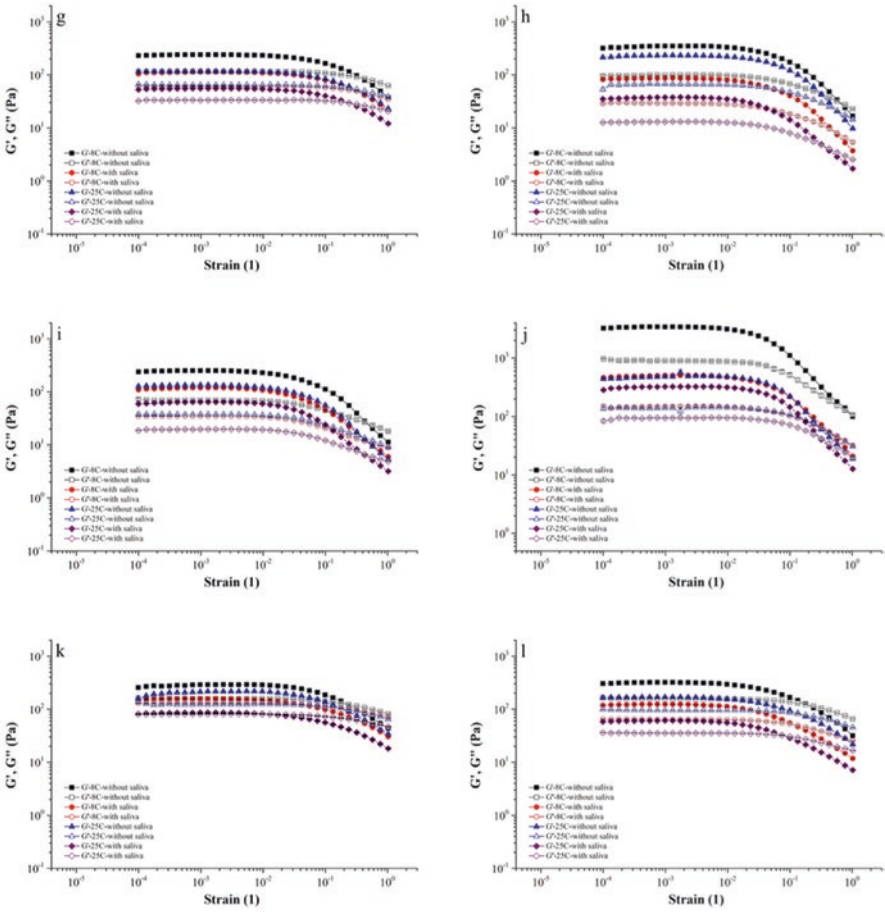

Fig. 12 (continued)

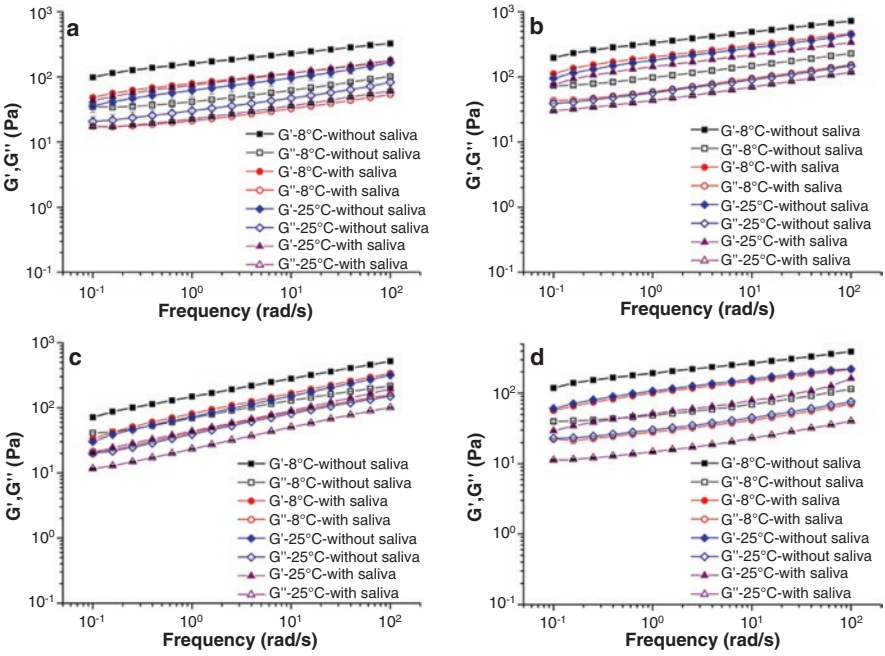

Fig. 13 Yogurt frequency sweep results; (**a**) sample 3; (**b**) sample 5; (**c**) sample 7; (**d**) sample 9

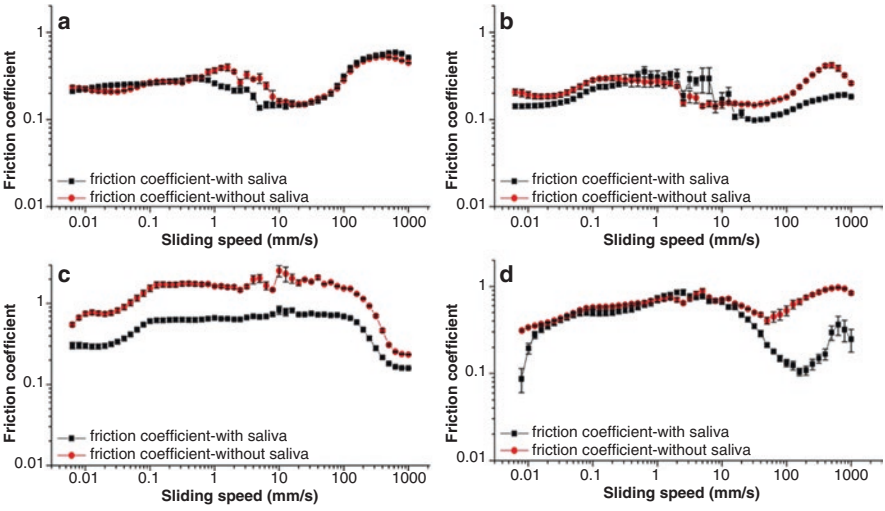

Fig. 14 Yogurt tribological profiles; (**a**) sample 2; (**b**) sample 3; (**c**) sample 5; (**d**) sample 11

References

Alakali, J., Okonkwo, T., & Iordye, E. (2008). Effect of stabilizers on the physico-chemical and sensory attributes of thermized yoghurt. *African Journal of Biotechnology, 7*(2), 158–163.

Andrewes, P., Kelly, M., Vardhanabhuti, B., & Foegeding, E. (2011). Dynamic modelling of whey protein–saliva interactions in the mouth and relation to astringency in acidic beverages. *International Dairy Journal, 21*(8), 523–530.

Berk, Z. (2018). *Food process engineering and technology*. London: Academic Press.

Bird, A. R., Brown, I. L., & Topping, D. L. (2000). Starches, resistant starches, the gut microflora and human health. *Current Issues in Intestinal Microbiology, 1*(1), 25–37.

Bongaerts, J., Fourtouni, K., & Stokes, J. (2007). Soft-tribology: Lubrication in a compliant PDMS–PDMS contact. *Tribology International, 40*(10), 1531–1542.

Bongaerts, J., Rossetti, D., & Stokes, J. (2007). The lubricating properties of human whole saliva. *Tribology Letters, 27*(3), 277–287.

Chen, J. (2015). Food oral processing: Mechanisms and implications of food oral destruction. *Trends in Food Science & Technology, 45*(2), 222–228.

Chen, J., & Engelen, L. (2012). *Food oral processing: Fundamentals of eating and sensory perception*. Chichester: Wiley.

Cho, S. S., & Prosky, L. (1999). Application of complex carbohydrates to food product fat mimetics. In *Complex carbohydrates in foods* (Food science and rechnology) (Vol. 93, pp. 411–430). New York: Marcel Dekker.

Chojnicka-Paszun, A., De Jongh, H., & De Kruif, C. (2012). Sensory perception and lubrication properties of milk: Influence of fat content. *International Dairy Journal, 26*(1), 15–22.

Dang, H. V., Loisel, C., Desrumaux, A., & Doublier, J. (2009). Rheology and microstructure of cross-linked waxy maize starch/whey protein suspensions. *Food Hydrocolloids, 23*(7), 1678–1686.

De Vicente, J., Stokes, J., & Spikes, H. (2006). Soft lubrication of model hydrocolloids. *Food Hydrocolloids, 20*(4), 483–491.

De Wijk, R., Terpstra, M., Janssen, A., & Prinz, J. (2006). Perceived creaminess of semi-solid foods. *Trends in Food Science & Technology, 17*(8), 412–422.

De Wijk, R. A., Kapper, C., Borsboom, P., & Prinz, J. F. (2009). Persistence of oral coatings of CMC and starch-based custard desserts. *Food Hydrocolloids, 23*(3), 896–900.

Genovese, D., Lozano, J., & Rao, M. A. (2007). The rheology of colloidal and noncolloidal food dispersions. *Journal of Food Science, 72*(2), R11–R20.

Guinard, J.-X., Zoumas-Morse, C., & Walchak, C. (1997). Relation between parotid saliva flow and composition and the perception of gustatory and trigeminal stimuli in foods. *Physiology & Behavior, 63*(1), 109–118.

Hansen, P. (1993). *Food hydrocolloids: Structures, properties and functions. Food hydrocolloids in the dairy industry*. New York: Plenum Press.

Hoover, R. (2001). Composition, molecular structure, and physicochemical properties of tuber and root starches: A review. *Carbohydrate Polymers, 45*(3), 253–267.

Huc, D., Michon, C., Bedoussac, C., & Bosc, V. (2016). Design of a multi-scale texture study of yoghurts using rheology, and tribology mimicking the eating process and microstructure characterisation. *International Dairy Journal, 61*, 126–134.

Humphrey, S. P., & Williamson, R. T. (2001). A review of saliva: Normal composition, flow, and function. *The Journal of Prosthetic Dentistry, 85*(2), 162–169.

Isleten, M., & Karagul-Yuceer, Y. (2006). Effects of dried dairy ingredients on physical and sensory properties of nonfat yogurt. *Journal of Dairy Science, 89*(8), 2865–2872.

Janssen, A. M., Terpstra, M. E., De Wijk, R. A., & Prinz, J. F. (2007). Relations between rheological properties, saliva-induced structure breakdown and sensory texture attributes of custards. *Journal of Texture Studies, 38*(1), 42–69.

Johnson, S., Gorman, D., Adams, M., & Briscoe, B. (1993). The friction and lubrication of human stratum corneum. *Tribology Series, 25*, 663–672. Elsevier.

Joyner, H. S., Pernell, C. W., & Daubert, C. R. (2014). Impact of formulation and saliva on acid milk gel friction behavior. Journal of food science, 79(5), E867–E880.

Karam, M. C., Gaiani, C., Hosri, C., Burgain, J., & Scher, J. (2013). Effect of dairy powders fortification on yogurt textural and sensorial properties: A review. *Journal of Dairy Research, 80*(4), 400–409.

Krzeminski, A., Großhable, K., & Hinrichs, J. (2011). Structural properties of stirred yoghurt as influenced by whey proteins. *LWT-Food Science and Technology, 44*(10), 2134–2140.

Laverse, J., Mastromatteo, M., Frisullo, P., Albenzio, M., Gammariello, D., & Del Nobile, M. (2011). Fat microstructure of yogurt as assessed by X-ray microtomography. *Journal of Dairy Science, 94*(2), 668–675.

Lee, W., & Lucey, J. (2004). Structure and physical properties of yogurt gels: Effect of inoculation rate and incubation temperature. *Journal of Dairy Science, 87*(10), 3153–3164.

Lee, W., & Lucey, J. (2010). Formation and physical properties of yogurt. *Asian-Australasian Journal of Animal Sciences, 23*(9), 1127–1136.

Lee, W.-J., & Lucey, J. (2006). Impact of gelation conditions and structural breakdown on the physical and sensory properties of stirred yogurts. *Journal of Dairy Science, 89*(7), 2374–2385.

Lucey, J., & Singh, H. (1997). Formation and physical properties of acid milk gels: A review. *Food Research International, 30*(7), 529–542.

Lucey, J., Tamehana, M., Singh, H., & Munro, P. (1998). A comparison of the formation, rheological properties and microstructure of acid skim milk gels made with a bacterial culture or glucono-δ-lactone. *Food Research International, 31*(2), 147–155.

Malone, M., Appelqvist, I., & Norton, I. (2003). Oral behaviour of food hydrocolloids and emulsions. Part 1. Lubrication and deposition considerations. *Food Hydrocolloids, 17*(6), 763–773.

Martin, N., Skokanova, J., Latrille, E., Beal, C., & Corrieu, G. (1999). Influence of fermentation and storage conditions on the sensory properties of plain low fat stirred yogurts. *Journal of Sensory Studies, 14*(2), 139–160.

Miller, J. L., & Watkin, K. L. (1996). The influence of bolus volume and viscosity on anterior lingual force during the oral stage of swallowing. *Dysphagia, 11*(2), 117–124.

Morell, P., Chen, J., & Fiszman, S. (2016). The role of starch and saliva in tribology studies and the sensory perception of protein-added yogurts. *Food & Function, 8*(2), 545–553.

Morell, P., Hernando, I., Llorca, E., & Fiszman, S. (2015). Yogurts with an increased protein content and physically modified starch: Rheological, structural, oral digestion and sensory properties related to enhanced satiating capacity. *Food Research International, 70*, 64–73.

Murray, B. S., & Phisarnchananan, N. (2014). The effect of nanoparticles on the phase separation of waxy corn starch+ locust bean gum or guar gum. *Food Hydrocolloids, 42*, 92–99.

Nguyen, P. T., Kravchuk, O., Bhandari, B., & Prakash, S. (2017). Effect of different hydrocolloids on texture, rheology, tribology and sensory perception of texture and mouthfeel of low-fat pot-set yoghurt. *Food Hydrocolloids, 72*, 90–104.

Ognean, C. F., Darie, N., & Ognean, M. (2006). Fat replacers: Review. *Journal of Agroalimentary Processes and Technologies, 12*(2), 433–442.

Official Methods of Analysis of AOAC INTERNATIONAL (1995a) AOAC INTERNATIONAL, Gaithersburg, MD, USA, Official Method 989.05

Official Methods of Analysis of AOAC INTERNATIONAL (1995b) AOAC INTERNATIONAL, Gaithersburg, MD, USA, Official Method 923.03

Official Methods of Analysis of AOAC INTERNATIONAL (1999) , AOAC INTERNATIONAL, Gaithersburg, MD, USA, Official Method 934.01

Pascua, Y., Koç, H., & Foegeding, E. A. (2013). Food structure: Roles of mechanical properties and oral processing in determining sensory texture of soft materials. *Current Opinion in Colloid & Interface Science, 18*(4), 324–333.

Peng, X., & Yao, Y. (2017). Carbohydrates as fat replacers. *Annual Review of Food Science and Technology, 8*, 331–351.

Perrechil, F., Braga, A., & Cunha, R. (2009). Interactions between sodium caseinate and LBG in acidified systems: Rheology and phase behavior. *Food Hydrocolloids, 23*(8), 2085–2093.

Prakash, S., Tan, D. D. Y., & Chen, J. (2013). Applications of tribology in studying food oral processing and texture perception. *Food Research International, 54*(2), 1627–1635.

Saint-Eve, A., Kora, E. P., & Martin, N. (2004). Impact of the olfactory quality and chemical complexity of the flavouring agent on the texture of low fat stirred yogurts assessed by three different sensory methodologies. *Food Quality and Preference, 15*(7), 655–668.

Sano, H., Egashira, T., Kinekawa, Y., & Kitabatake, N. (2005). Astringency of bovine milk whey protein. *Journal of Dairy Science, 88*(7), 2312–2317.

Sarkar, A., & Singh, H. (2012). Oral behaviour of food emulsions. In *Food oral processing* (pp. 111–137). Oxford: Wiley-Blackwell.

Serra, M., Trujillo, A. J., Quevedo, J. M., Guamis, B., & Ferragut, V. (2007). Acid coagulation properties and suitability for yogurt production of cows' milk treated by high-pressure homogenisation. International Dairy Journal, 17(7), 782–790.

Singh, N., Singh, J., Kaur, L., Sodhi, N. S., & Gill, B. S. (2003). Morphological, thermal and rheological properties of starches from different botanical sources. *Food Chemistry, 81*(2), 219–231.

Sonne, A., Busch-Stockfisch, M., Weiss, J., & Hinrichs, J. (2014). Improved mapping of in-mouth creaminess of semi-solid dairy products by combining rheology, particle size, and tribology data. *LWT-Food Science and Technology, 59*(1), 342–347.

Stokes, J. R., Boehm, M. W., & Baier, S. K. (2013). Oral processing, texture and mouthfeel: From rheology to tribology and beyond. *Current Opinion in Colloid & Interface Science, 18*(4), 349–359.

Tang, C.-H., & Liu, F. (2013). Cold, gel-like soy protein emulsions by microfluidization: Emulsion characteristics, rheological and microstructural properties, and gelling mechanism. *Food Hydrocolloids, 30*(1), 61–72.

Thaiudom, S., & Goff, H. (2003). Effect of κ-carrageenan on milk protein polysaccharide mixtures. *International Dairy Journal, 13*(9), 763–771.

van de Velde, F., de Hoog, E. H., Oosterveld, A., & Tromp, R. H. (2015). Protein-polysaccharide interactions to alter texture. *Annual Review of Food Science and Technology, 6*, 371–388.

Vingerhoeds, M. H., Silletti, E., De Groot, J., Schipper, R. G., & Van Aken, G. A. (2009). Relating the effect of saliva-induced emulsion flocculation on rheological properties and retention on the tongue surface with sensory perception. *Food Hydrocolloids, 23*(3), 773–785.

Zinoviadou, K., Janssen, A., & De Jongh, H. (2008). Tribological properties of neutral polysaccharide solutions under simulated oral conditions. *Journal of Food Science, 73*(2), E88–E94.